

The Economic Geography of Global Warming

JOSÉ-LUIS CRUZ

University of California, Berkeley

and

ESTEBAN ROSSI-HANSBERG

University of Chicago

First version received October 2021; Editorial decision January 2023; Accepted March 2023 (Eds.)

Global warming is a worldwide and protracted phenomenon with heterogeneous local economic effects. We propose a dynamic economic assessment model of the world economy with high spatial resolution to assess its consequences. Our model features several forms of adaptation to local temperature changes, including costly trade and migration, local technological innovations, and local natality rates. We quantify the model at a $1^\circ \times 1^\circ$ resolution and estimate damage functions that determine the impact of temperature changes on a region's fundamental productivity and amenities conditional on local temperatures. Welfare losses from global warming are very heterogeneous across locations, with 20% losses in parts of Africa and Latin America but also gains in some northern latitudes. Overall, spatial inequality increases. Uncertainty about average welfare effects is significant but much smaller for relative losses across space. Migration and innovation are shown to be important adaptation mechanisms. We use the model to study the impact of carbon taxes, abatement technologies, and clean energy subsidies. Carbon taxes delay consumption of fossil fuels and help *flatten the temperature curve* but are much more effective when an abatement technology is forthcoming.

Key words: carbon taxes, climate change, environmental policy, integrated assessment models, spatial growth, migration, trade

JEL Codes: F63, F64, Q51, Q54, Q56

1. INTRODUCTION

Carbon emissions generated by the economic activity of humans are warming the planet. They will affect temperatures everywhere on Earth over long periods of time and in geographically heterogeneous ways. What will be the impact of carbon emissions, and the implied changes in temperatures, on the world economy and on the economy of particular

The editor in charge of this paper was Thomas Chaney.

regions? How will individuals react to these changes and how are these reactions impacted by their ability to migrate, trade, or invest and develop alternative centers of economic activity? What are the best policies to combat global warming and what are their implications for different regions across the world? In this paper, we propose and quantify a novel global spatial dynamic assessment model to address these questions.

The nature of the global warming phenomenon determines the elements of our assessment model. Global carbon emissions affect local temperatures around the world, so we want a model of the world economy. Because these effects are extremely heterogeneous across regions, even within countries, we want a model with local geographic detail where temperatures affect both productivity and the living amenities from residing in particular locations. Agents facing adverse temperature conditions that affect their welfare in a given location will react by moving, by trading with other locations, and by developing centers of economic activity in areas that are not so heavily affected or that benefit from warmer temperatures. Hence, we require a model with costly trade and migration, as well as private technological investments. We also need to introduce clean and carbon-based energy as inputs in production so that fossil fuels create carbon dioxide emissions, which in turn affect global and local temperatures through a global carbon cycle and a temperature down-scaling model. Because global warming is a protracted phenomenon developing over hundreds of years and happening in a growing economy, we need an assessment model that is dynamic and incorporates the implications of this growth on carbon emissions and adaptation over time. Such a model will also allow us to study and understand the dynamic implications of this phenomenon across locations. Once we incorporate dynamics over long periods of time, we also need to incorporate population changes by means of birth and mortality rates that vary across regions with different incomes and temperatures.

Our starting point is the spatial growth framework in [Desmet et al. \(2018\)](#). We model trade, migration, and innovation as in that paper. We add clean and carbon-based energy as inputs in production with imperfect substitutability, a carbon extraction technology with costs that depend on the cumulative total stock of carbon extracted, and an associated carbon cycle that determines global temperature and, through a local down-scaling factor, local temperatures. We model the effect of local temperature on fundamental productivities and amenities through two distinct damage functions that determine the impact of temperature changes on each local characteristic, as a function of the current temperature. The estimated functions indicate, as expected although not imposed, that warm regions' productivities and amenities are impacted negatively by increases in temperatures, while the opposite is the case for the coldest regions. We also incorporate fertility into the model, so that in every period agents living at a particular location have a natality rate (birth minus death rate) that depends on their income and the local temperature. This adds local and global population dynamics to our model.

We quantify the model devoting particular attention to identifying the effect that changes in local climatic conditions have on local productivities and amenities. We start by using data from G-Econ, the Human Development Index, together with a number of parameters obtained from the literature, to invert the model and obtain the local productivities and amenities that rationalize populations and income every five year-period from 1990 to 2005 (the years for which G-Econ is available). This model inversion also yields the migration costs that rationalize population movements across regions given the natality function we estimate using the United Nations net natality rates. We then use the fundamental productivities and amenities to estimate how they are affected by changes in local temperatures. Because these fundamental productivities and

amenities come from a model with costly trade, migration, innovation, and fertility, these adaptation mechanisms are already taken explicitly into account. This is clearly preferable to estimating damage functions from endogenous outcomes like output or population and, as we show, yields clearer and more precise results. We estimate the effect of climate on these fundamentals allowing for the semi-elasticity to depend on local temperature and include location and time fixed effects as well as regional trends. The estimated damage functions yield significant effects of changes in temperature for wide ranges of initial current temperatures, but they also yield relatively large confidence intervals that we use to assess the uncertainty underlying our results.¹

The final step in the quantification is to parameterize the effect of carbon use for future carbon extraction costs and the carbon cycle. We model energy as a constant elasticity of substitution composite between fossil fuels and clean energy. The cost of these two sources of energy evolves with the world's endogenous technology, but the cost of fossil fuels also depends on the amount of carbon that has been used in the past, since the remaining stock is increasingly harder to extract. Using data from [Bauer et al. \(2017\)](#), we estimate a convex relationship between cumulative emissions and the cost of extraction. Firms decide on their use of fossil fuels, which leads to carbon emissions. A standard carbon cycle model (as in [IPCC, 2013](#)) then generates global temperature dynamics.² Our baseline analysis matches the global temperature dynamics from 2000 to 2400 in the IPCC RCP 8.5 or 6.0 scenarios, depending on the calibration of the carbon cycle, almost exactly. To down-scale from global to local temperatures we follow [Mitchell \(2003\)](#) and use a linear function with heterogeneous local factors that we estimate as a function of a large number of local characteristics. The estimated down-scaling factors (the local temperature change for a one-degree change in global temperature) can be as large as 2.2 in parts of Siberia and Alaska and as low as 0.5 in parts of Asia and South America.

With the quantified model in hand, we can simulate the economy forward over several centuries and evaluate the economic consequences of global warming under both carbon cycle calibrations (RCP 8.5 and 6.0). Global warming is expected to have heterogeneous effects over space, where the hottest regions in South America, Africa, India, and Australia experience welfare losses of 20% for RCP 8.5 (4% for RCP 6.0), and the coldest regions in Alaska, Northern Canada, and Siberia undergo welfare gains as high as 11% (4%). On average, the world is expected to lose around 6% (1%) in terms of welfare, although the exact number depends on the yearly discount factor.³ Global warming increases inequality across space. Welfare losses across locations are negatively correlated with current real income per capita and welfare. The poorest regions of the world, mainly located in Sub-Saharan Africa and South East Asia, are the ones undergoing the highest warming losses. By 2200, the average loss in welfare is 10% (2%) and in output is 5% (1%), although the uncertainty inherited from our estimated damage functions implies that the 95% confidence intervals include losses as high as 20% (6%) and 12% (3%), respectively. The large uncertainty in average outcomes, however, does not translate into significant uncertainty about the spatial distribution of losses. The

1. Our results are robust to alternative formulations that also incorporate changes in extreme weather patterns and sectoral composition through the local share of agriculture in value added.

2. We also include exogenous CO₂ emissions from forestry and non-CO₂ greenhouse gasses from RCP 8.5 or 6.0.

3. In our baseline scenario we use a discount factor of $\beta=0.965$ in an economy where real GDP grows by around 3% per year.

relative distribution of losses is similar in our baseline case compared to the worst- or the best-case scenarios (as measured by the 95% confidence intervals of our damage functions). When we decompose the losses coming from the effect of global warming on amenities or productivity, we find that about half of the average effects come from the impact of temperature rise on productivity. Effects on amenities are particularly important for losses in Africa and gains at the most northern latitudes; while losses in productivity affect almost all regions to the south of the 30° latitude.

Our evaluation of the effects of global warming underscores economic adaptation through migration, trade, and endogenous local innovation. We assess the importance of each of these adaptation channels using counterfactuals that increase the cost of migrating, trading, or investing by a certain percentage globally. If we increase migration costs by 25% throughout the globe, the average cost of global warming rises by an additional 3% by the year 2200. Higher migration costs make global warming more costly for Africa where migration serves as a safety valve that keeps wages from falling too much, but also for northern regions that now benefit less from the influx of migrants. Increases in migration costs lead to significantly faster population growth as more people stay in poorer areas where they have more children. To understand the effect of potential policy reactions to climate migrants, we also study a case where we increase the specific cost of migrating out of Africa. This counterfactual makes global warming not only more costly in Africa itself, but also in the rest of the world.

Compared to migration, we find a substantially smaller impact from increases in trade costs. The reason is that the evolution of temperature is spatially correlated, and most trade is local. Furthermore, our model features trade, but only an aggregate sector and therefore no adaptation through sectoral specialization.⁴ The role of innovation is between those of migration and trade; a rise in innovation costs has a large relative effect that benefits the coldest places but hurts the warmest ones significantly. On average, though, higher innovation costs imply that regions in India and China, which will eventually be heavily affected by global warming, grow less and so the world on average loses less from the rise in temperatures due to a reallocation of population towards northern latitudes.

The last part of the paper uses our quantified model to evaluate a number of environmental policies. The equilibrium allocation in the modeled economy is not efficient due to carbon emissions being a global externality, but also due to the presence of production externalities, technology diffusion, and congestion externalities. We study taxes on carbon dioxide, subsidies for clean energy, and the importance of abatement technologies that eliminate the pernicious effects of carbon. Clean energy subsidies have only a modest effect on carbon emissions and the corresponding evolution of global temperature. Although they generate substitution towards clean energy, they also lead to a reduction in the price of energy which translates into more production and ultimately more energy use. These effects tend to cancel each other out.

Carbon taxes have a larger effect on CO₂ emissions and temperatures. The reduction in the use of fossil fuels leads to fewer carbon emissions which results in lower temperatures that persist for hundreds of years. However, the reduction in carbon

4. We incorporate the role of heterogeneity across economic sectors by allowing the damage function to vary according to the share of value added in agriculture. When we do so, we find a similar spatial pattern of losses. Further details are provided in [Online Appendix B.3](#). [Conte et al. \(2021, 2022\)](#) develop a related model that incorporates an agricultural and a non-agricultural sector and where trade plays a more important role as an adaptation mechanism.

use also implies that more carbon is left unexploited on Earth, which yields lower future extraction costs. The implication is that carbon taxes primarily *delay* the use of the carbon, rather than decreasing its total use. This has the effect of *flattening* the temperature curve, with lower temperatures for long periods of time, but with little impact over the very long-run. Hence, the effects of carbon taxes on the environment are primarily concentrated in the next 100 years or so. Using *ad-valorem* or excise taxes does not alter this implication but, naturally, proportional taxes that increase rapidly over time can help reduce the total amount of carbon used. Of course, this result also implies that carbon taxes can be particularly effective in combination with abatement technologies. If abatement technologies are forthcoming, delaying carbon consumption has tremendously positive effects since the effect of future emissions is abated using the new technology. Thus, our results strongly suggest that carbon taxes should be combined with incentives to invent effective abatement technologies. To use an analogy from the epidemiology literature, flattening an infection curve is particularly effective if a cure is forthcoming, but much less so otherwise.⁵

Standard models of global warming use aggregate loss functions that relate the future path of the aggregate economy to the evolution of climate variables. In many cases, these functions fail to incorporate, or do so in only a reduced-form way, the behavioral responses of individuals and firms. Because those functions are not derived from micro-founded models in which optimal behavior is obtained as a response to climatic shocks, they fail to consider that households and firms can adapt, although bearing costs, to the most salient consequences of this phenomenon. Incorporating these responses is particularly important because of the vast heterogeneity that rising temperatures will have on the fundamentals of the economy. It is also essential because only a model that explicitly takes into account these behavioral adaptation responses across regions can properly account for potential changes in aggregate loss functions in policy counterfactuals and simulations of alternative scenarios (an expression of the Lucas critique, Lucas, 1976). A quantitative dynamic model like ours, with individual behavioral responses and explicit treatment of spatial heterogeneity at a high resolution, is a needed addition to the economics of climate change.

In the last decade, there has been a surge of empirical estimates of climate damages that use panel methodologies and exploit short-run weather variation to identify the causal effect of temperature on economic and social outcomes.⁶ This work has been useful to provide evidence of the link between temperature and economic outcomes, but it

5. As we know from standard Pigouvian analysis, we can address the negative externality created by fossil fuels using taxes that increase their price. However, another potentially effective strategy is to increase the elasticity of substitution between fossil fuels and clean sources in the technology to produce energy (Cruz and Rossi-Hansberg, 2022). In the aggregate, this elasticity is not a fundamental parameter of technology, but rather a parameter that aggregates the many ways the world has to produce energy. As such, this parameter is not necessarily either constant or policy invariant. Although we use estimates in the literature and fix it at 1.6 in our baseline scenario, we show that increases in this elasticity can be extremely effective in reducing the use of fossil fuels over time as extraction costs rise. Such an increase in this elasticity can be achieved, for example, by switching vehicles to use energy from all sources, as electric cars do.

6. This wave of empirical papers was pioneered by the work of Deschênes and Greenstone (2007), who study the impact of temperature on agricultural profits. This methodology has been employed to quantify the weather effects on mortality (Barreca et al., 2016; Carleton et al., 2022), amenities (Albouy et al., 2016; Baylis, 2020), crime and conflict (Burke et al., 2015a), migration (Missirian and Schlenker, 2017), crop yields (Schlenker and Roberts, 2009), and GDP and GDP growth (Dell et al., 2012; Burke et al., 2015b). Dell et al. (2014) and Auffhammer (2018) review this body of research.

cannot be used to determine the future effects of temperature across regions or to evaluate different policies. Since our estimation strategy of the impact of local temperature on amenities and productivity explicitly controls for migration, trade, and innovation as long-run adaptation mechanisms, and it estimates the effects non-parametrically by temperature bin, it represents a new approach within the *Climate Adaptive Response Estimation* literature ([Auffhammer, 2018](#)).

Some of these estimates have been incorporated into economic models of global warming, also known as Integrated Assessment Models (IAM), to quantify their economic consequences. The most popular models tend to consider coarse geographical units and display a limited role for adaptation mechanisms in mediating climate damages ([Nordhaus, 2017](#); [Anthoff and Tol, 2014](#); [Hope and Hope, 2013](#); [IPCC, 2013](#); [Golosov et al., 2014](#)). A notable exception is [Krusell and Smith \(2022\)](#), who consider a spatial resolution similar to ours but, in contrast to us, consider the effect of global warming on local capital investments. We depart from their work, by explicitly incorporating trade, migration, innovation, and population growth, and by estimating the damage functions on productivities and amenities, rather than GDP.⁷

We contribute to the development of IAMs by incorporating recent developments in spatial quantitative models. In particular, we build on [Desmet et al. \(2018\)](#), that develops a spatial growth theory at a fine level of geographical resolution and analyzes the evolution of the economy over several centuries. The static spatial component resembles [Allen and Arkolakis \(2014\)](#), but adds costly migration, and the dynamic component follows [Desmet and Rossi-Hansberg \(2014\)](#).⁸ We incorporate local fertility and population dynamics, energy use, fossil fuels extraction costs, a carbon cycle, effects of temperature on productivity and amenities, among other features to these existing economic frameworks.

There is an incipient literature of spatial IAMs (or S-IAMs), that addresses environmental questions through the lens of spatial dynamic models. [Balboni \(2021\)](#) quantifies the cost of road investment in the coasts of Vietnam under the presence of sea level rise. [Desmet et al. \(2021\)](#) measures the spatial shifts in population and economic activity due to sea level rise, using a highly spatially disaggregated model, closer to ours. [Desmet and Rossi-Hansberg \(2015\)](#), [Nath \(2020\)](#), [Conte et al. \(2021, 2022\)](#), and [Cruz \(2021\)](#) evaluate the impact of global warming across different economic sectors which is something we do not incorporate in this paper. Relative to them, we add realistic spatial heterogeneity, dynamics and high spatial resolution, and population dynamics and effects of temperature on amenities, respectively. Ultimately, our aim is to propose a quantitative model with all the necessary elements to serve as a workhorse for a new

7. These core models have been extended to analyze different dimensions of global warming. [Popp \(2004\)](#), [Acemoglu et al. \(2012, 2016, 2020\)](#), and [Hassler et al. \(2019\)](#) assess the role of clean technology investments and innovations in mitigating climate damages. [Benveniste et al. \(2020\)](#) explores the extent to which migration and border policies attenuate the level of exposure and vulnerability to climate change impacts. [Dietz and Lanz \(2019\)](#) studies the capacity to meet food demand for different climate change conditions. [Fried \(2022\)](#) evaluates the role of investment in adaptation capital to reduce damages from extreme weather. [Hassler et al. \(2018\)](#) compares warming-induced losses in GDP and optimal carbon taxes, when considering extreme values for the climate sensitivity and economic damages. [Costinot et al. \(2016\)](#) examines the losses in the agriculture sector when trade and production patterns are allowed to adjust across different crops. [Barrage \(2019\)](#) studies the optimal environmental policy in the presence of distortionary taxes.

8. See [Redding and Rossi-Hansberg \(2017\)](#) for a survey of this literature.

generation of IAM models that incorporate dynamics, rich spatial heterogeneity, and micro-founded adaptation mechanisms.

The rest of the paper is structured as follows. Section 2 presents the economic and climate model. Section 3 quantifies the model and estimates the damage functions. Section 4 describes the baseline quantitative implications of global warming. Section 5 discusses the role of the different forms of adaptation in mediating the harmful effects of global warming. Section 6 analyzes the effect of a number of environmental policies. Section 7 concludes. An [Online Appendix](#) includes details of our data, derivations, robustness checks, additional exercises and extensions. Additional materials are included in a [Supplementary Materials Section](#).

2. THE MODEL

The economic component of the model extends [Desmet et al. \(2018\)](#) among a number of dimensions. First, we incorporate an endogenous law of motion for global population. Second, we consider that production requires labor, land, and energy. Energy comes from fossil fuels or clean sources. The former type of energy generates CO₂ emissions, whereas the latter does not. Third, local climate conditions distort the fundamental amenities, productivities, and natality rates in spatially heterogeneous ways.

The carbon cycle and the global temperature modules are based on the reduced-form models in [IPCC \(2013\)](#). The projection from global to local temperature follows the statistical down-scaling approach, formalized by [Mitchell \(2003\)](#).

2.1. Endowment and Preferences

The world economy occupies a two-dimensional surface S , where a location is defined as a point $r \in S$ with land density $H(r)$. In each period t , L_t agents live in the world economy. Global population is time-dependent due to endogenous natality rates.

Every period, agents derive utility from consuming a set of differentiated varieties $c_t^\omega(r)$ aggregated according to a CES utility function, from local amenities, $b_t(r)$, and from their idiosyncratic preference for the location where they live, $\varepsilon_t^i(r)$. If agents move from r to s at t , utility is discounted by mobility costs, $m(r, s)$, which are paid as a permanent flow cost from t onward. Specifically, the period utility of agent i who resides in r in period t and has a location history $r_- = (r_0, \dots, r_{t-1})$ is given by

$$u_t^i(r_-, r) = \left[\int_0^1 c_t^\omega(r)^\rho d\omega \right]^{\sigma/\rho} b_t(r) \varepsilon_t^i(r) \prod_{s=1}^t m(r_{s-1}, r_s)^{-1}.$$

Agents earn income from work. They inelastically supply one unit of labor and receive a wage $w_t(r)$. They also receive a share of land rents, $H(r)R_t(r)$, which are uniformly distributed across a location's residents. Thus, per capita real income is $y_t(r) = (w_t(r) + R_t(r)/L_t(r))/P_t(r)$, where $L_t(r)$ denotes local population density (population per unit of land) and $P_t(r)$ the local ideal CES price index. The parameter σ governs the curvature in the utility function which determines the elasticity of utility to real income.

Local amenities $b_t(r)$ are affected by congestion according to $b_t(r) = \bar{b}_t(r)L_t(r)^{-\lambda}$, where $\bar{b}_t(r)$ represents a location's *fundamental* amenities and λ the congestion elasticity of amenities to population density. Fundamental amenities can be distorted by local climate conditions through the *damage* function $\Lambda^b(\cdot)$. This function denotes the

percentage change in fundamental amenities when local temperature rises from $T_{t-1}(r)$ in period $t-1$ to $T_t(r) = \Delta T_t(r) + T_{t-1}(r)$ in period t . Namely,

$$\bar{b}_t(r) = \left(1 + \Lambda^b(\Delta T_t(r), T_{t-1}(r))\right) \bar{b}_{t-1}(r). \quad (2.1)$$

Hence, when $\Lambda^b(\Delta T_t(r), T_{t-1}(r))$ is negative (positive), amenities in cell r are damaged (improved) by increases in local temperature. The dependence of the damage function on the level of temperature, and not only on the change in temperature, captures the heterogeneous impacts over space that global warming is expected to have. Naturally, and as we estimate in Section 3, the amenities in hot places (like Congo) decline with further increases in temperature, whereas amenities in cold places (like Siberia) benefit from warmer climate.

Households also experience idiosyncratic taste shocks, $\varepsilon_t^i(r)$, that we assume are independent and identically distributed across households, locations, and time according to a Fréchet distribution with shape parameter $1/\Omega$ and scale parameter 1. A greater value of Ω implies more dispersion in agent's tastes across locations, acting as a second congestion force.

We assume that the flow-utility cost of moving from r to s is given by the product of an origin-specific cost, $m_1(r)$, and a destination-specific cost, $m_2(s)$, so $m(r, s) = m_1(r)m_2(s)$. Since staying in the same location is costless, $m(r, r) = 1$, origin costs are simply the inverse of destination costs, namely $m_1(r) = 1/m_2(r)$. Hence, the permanent utility cost of entering a location is compensated by a permanent utility benefit when leaving, which implies that agents only pay the flow cost while residing there. This way of modeling migration costs implies that migration decisions are reversible and, therefore, the location choice of agents only depends on current variables and not on past or future ones. As is standard in discrete choice models with idiosyncratic preferences, the fraction of households residing in r at period t is then given by

$$\frac{L_t(r)H(r)}{L_t} = \frac{u_t(r)^{1/\Omega} m_2(r)^{-1/\Omega}}{\int_S u_t(v)^{1/\Omega} m_2(v)^{-1/\Omega} dv}, \quad (2.2)$$

where $u_t(r)$ denotes the component of local utility that is not idiosyncratic, namely,

$$u_t(r) = b_t(r)y_t(r)^\sigma = b_t(r) \left[\int_0^1 c_t^\omega(r)^\rho d\omega \right]^{\sigma/\rho}. \quad (2.3)$$

At the end of period t , after the migration decisions have been made, each household has $n_t(r)$ net off-springs. Local natality rates are exogenous to the individual but endogenous to a location's real income and local temperature, $n_t(r) = \eta(y_t(r), T_t(r))$. Therefore, at the beginning of period $t+1$, before migration decisions are made, local population density $L'_{t+1}(r)$ is determined by $L'_{t+1}(r)H(r) = (1 + n_t(r))L_t(r)H(r)$.

Note that global population depends not only on the distribution of natality rates across space and time, and through them on the distribution of income and local temperatures, but also on the spatial distribution of population in the previous period.

2.2. Technology

In each cell there is a continuum of firms, producing differentiated varieties $\omega \in [0,1]$. Output is produced using a constant returns to scale technology in land, labor, and energy. Output per unit of land of variety ω is given by

$$q_t^\omega(r) = \phi_t^\omega(r)^{\gamma_1} z_t^\omega(r) \left(L_t^\omega(r)^\chi e_t^\omega(r)^{1-\chi} \right)^\mu, \quad (2.4)$$

where $L_t^\omega(r)$ and $e_t^\omega(r)$ denote the production workers and the energy use, both per unit of land. Note that, since land is a fixed factor with share $1-\mu$, agglomerating labor and energy in a location yields decreasing returns, which acts as a third congestion force.

A firm's productivity is determined by its innovation decision, $\phi_t^\omega(r) \geq 1$, and an idiosyncratic location-variety productivity shifter, $z_t^\omega(r)$. Firms can invest in innovation by paying a cost $\nu \phi_t^\omega(r)^\xi$ per unit of land, expressed in units of labor. The exogenous productivity shifter is the realization of a random variable which is independent and identically distributed across varieties and time according to a Fréchet distribution with cumulative distribution function $F(z, a) = e^{-a_t(r)z^{-\theta}}$. The scale parameter $a_t(r)$ governs the level of productivity in a location and is affected by agglomeration externalities as a consequence of high population density and endogenous past innovations. In particular, we let $a_t(r) = \bar{a}_t(r) L_t(r)^\alpha$ where α governs the strength of the first agglomeration force.

In turn, fundamental productivity, $\bar{a}_t(r)$, is determined by an endogenous dynamic process given by

$$\bar{a}_t(r) = (1 + \Lambda^a(\Delta T_t(r), T_{t-1}(r))) \left(\phi_{t-1}(r)^{\theta\gamma_1} \left[\int_S D(v, r) \bar{a}_{t-1}(v) dv \right]^{1-\gamma_2} \bar{a}_{t-1}(r)^{\gamma_2} \right). \quad (2.5)$$

Equation (2.5) has four components. The term $\phi_{t-1}(r)^{\theta\gamma_1}$ represents the shift in the local distribution of shocks that results from last period's innovation decisions of firms, which are assumed to now be embedded in the local technology.⁹ The individual contemporaneous effect of innovation affects the production function in (2.4) directly. The term $\left[\int_S D(v, r) \bar{a}_{t-1}(v) dv \right]^{1-\gamma_2} \bar{a}_{t-1}(r)^{\gamma_2}$ denotes the level of past technology that firms build on. It is composed of the location's own technology level $\bar{a}_{t-1}(r)$, as well as technology diffusion from other locations, where the function $D(v, r)$ denotes the spatial decay in the strength of technology diffusion. This specification follows Desmet et al. (2018) closely and all its dynamic implications are developed and discussed there. It generates a spatial endogenous growth model. Important for our purposes is that we add the term $\Lambda^a(\cdot)$, which incorporates the effect of temperature on local productivity. When the damage function $\Lambda^a(\Delta T_t(r), T_{t-1}(r))$ is negative (positive), productivity in cell r at time t declines (increases) due to temperature change. Since $\Lambda^a(\cdot)$ depends on temperature levels, it is flexible to capture the heterogeneous spatial impacts of global warming on productivity.

Unlike Desmet et al. (2018), production does not only require land and labor, but also energy. Following Golosov et al. (2014), Hassler et al. (2019), and Popp (2006), among

9. As Desmet et al. (2018) shows, all firms in a given location and point in time make identical innovation decisions.

others, energy and other factors are aggregated through a Cobb-Douglas production function where $(1-\chi)\mu$ denotes the share of energy in the production process. In turn, energy is a CES composite between fossil fuels, $e_t^{f,\omega}(r)$, and clean sources, $e_t^{c,\omega}(r)$, where the elasticity of substitution is given by ϵ .¹⁰ The use of fossil fuels generates CO₂ emissions, which accumulate in the atmosphere, intensifying the greenhouse gas effect, whereas the use of clean energy does not. Specifically, we let

$$e_t^\omega(r) = \left(\kappa e_t^{f,\omega}(r)^{\frac{\epsilon-1}{\epsilon}} + (1-\kappa) e_t^{c,\omega}(r)^{\frac{\epsilon-1}{\epsilon}} \right)^{\frac{\epsilon}{\epsilon-1}}, \quad (2.6)$$

where κ governs the relative productivity of both technologies in producing energy.

We assume competitive local energy markets and so the price of each type of energy is equal to its marginal production cost. Producing one unit of energy of type $j \in \{f, c\}$ requires $\mathcal{Q}_t^j(r)$ units of labor. The cost of energy varies across locations, time, and source, according to

$$\mathcal{Q}_t^f(r) = \frac{f(CumCO2_{t-1})}{\zeta_t^f(r)} \quad \text{and} \quad \mathcal{Q}_t^c(r) = \frac{1}{\zeta_t^c(r)}. \quad (2.7)$$

The evolution of the cost of fossil fuel, $\mathcal{Q}_t^f(r)$, is composed of two terms. The numerator denotes the cost of extracting fossil fuels from the ground, which we assume is increasing and convex in total world cumulative CO₂ emissions, $CumCO2_{t-1}$, following [Nordhaus and Boyer \(2002\)](#).¹¹ As cumulative emissions increase, carbon reserves shrink, which rises the cost of extraction. Cumulative emissions are simply the sum of cumulative emissions in the previous period plus the global CO₂ emissions released at t , E_t^f , namely

$$CumCO2_t = CumCO2_{t-1} + E_t^f = CumCO2_{t-1} + \int_S \int_0^1 e_t^{f,\omega}(v) H(v) d\omega dv. \quad (2.8)$$

The denominator of the energy price relates to the productivity, $\zeta_t^j(r)$, in energy generation of type j . We assume that the rate at which technology evolves over time in the fossil fuel and clean sector is related to global real GDP, y_t^w , which is endogenous in this model, as it depends on the investment decisions of firms. In particular, we consider that an increase of one percent in global real GDP rises log-productivity in energy generation by v^j , where this elasticity is allowed to vary across types of energy. That is,

$$\zeta_t^j(r) = \left(\frac{y_t^w}{y_{t-1}^w} \right)^{v^j} \zeta_{t-1}^j(r), \quad \text{where} \quad y_t^w = \int_S \left(\frac{L_t(v)H(v)}{L_t} \right) y_t(v) dv. \quad (2.9)$$

10. This elasticity governs the extent to which energy sources might not be perfect substitutes due to their ease of use, their location, or the existence of technologies and capital designed to primarily use a particular source. We introduce it as a fixed parameter, but perform a number of counterfactual exercises to assess its impact.

11. This amounts to assuming that fossil fuel markets are globally integrated such that, in equilibrium, marginal extraction costs are equal to the aggregate level (with the actual friction-less trade in fossil fuels left implicit).

Consequently, firm's innovations generate an externality on energy productivity improvements with magnitude that depends on the evolution of real GDP.¹²

We also assume that land markets are competitive. Firms bid for land and the firm whose bid is the largest wins the right to produce in that parcel. This is important since past innovations, embedded in the level of the local idiosyncratic distribution of productivities, benefit all potential entrants. As proven in [Desmet and Rossi-Hansberg \(2014\)](#), this implies that the solution to the dynamic innovation problem of firms is to simply choose the level of innovation that maximizes their current profits (or equivalently their bid for land), since all future gains of current innovations will accrue to land, which is the fixed factor. Future firms profits are zero independently of a firm's actions and so do not affect its decisions. Since there is a continuum of potential entrants, firms end up bidding all of their profits after covering innovation costs. Hence, in this economy, firm profits are zero and the maximum bid for land is the local land price, $R_t(r)$, every period. In sum, firms in r simply maximize

$$\begin{aligned} \max_{q, L, \phi, e^f, e^c} \quad & p_t^\omega(r, r) q_t^\omega(r) - w_t(r) L_t^\omega(r) - w_t(r) \nu \phi_t^\omega(r)^\xi \\ & - w_t(r) Q_t^f(r) e_t^{f, \omega}(r) - w_t(r) Q_t^c(r) e_t^{c, \omega}(r) - R_t(r) \end{aligned}$$

where $q_t^\omega(r)$ is given by (2.4) and (2.6), and $p_t^\omega(r, r)$ is the price at location r of variety ω produced at r .

The first order conditions with respect to fossil fuel and clean energy allow us to rewrite the total energy cost in labor units as the energy composite $e_t^\omega(r)$ times its ideal price index $Q_t(r)$. Namely, $Q_t(r) e_t^\omega(r) = Q_t^f(r) e_t^{f, \omega}(r) + Q_t^c(r) e_t^{c, \omega}(r)$, where $Q_t(r) = (\kappa^\epsilon Q_t^f(r)^{1-\epsilon} + (1-\kappa)^\epsilon Q_t^c(r)^{1-\epsilon})^{\frac{1}{1-\epsilon}}$. Since technology is Cobb-Douglas, a firm's energy costs are proportional to labor costs, so $Q_t(r) e_t^\omega(r) = \frac{1-\chi}{\chi} L_t^\omega(r)$. Thus, the problem of the firm collapses to a problem parallel to that in [Desmet et al. \(2018\)](#), and so all their results apply.

2.3. Prices, Export Shares, and Trade Balance

Goods markets are competitive, so firms sell goods at marginal cost after accounting for transport costs. Let $\varsigma(s, r) \geq 1$ denote the iceberg trade cost of shipping a good from r to s . Then, $p_t^\omega(s, r) = \varsigma(s, r) m_{c_t}(r) / z_t^\omega(r)$, where $m_{c_t}(r)$ denotes the marginal input cost at location r , which is common across firms since they face the same prices and therefore make the same decisions. The marginal input costs is given by $m_{c_t}(r) = \mathcal{M} Q_t(r)^{(1-\chi)\mu} w_t(r)^{\mu+\gamma_1/\xi} R_t(r)^{1-\mu-\gamma_1/\xi}$, where \mathcal{M} is a proportionality constant that depends on production parameters.

As is standard in trade structures based on [Eaton and Kortum \(2002\)](#), the probability, $\pi_t(s, r)$, that a good produced in r is consumed at s is then given by a gravity equation

12. An alternative approach would be to explicitly model the purposeful innovation decisions by firms that extract and distribute fossil fuels and generate clean energy, as we did for the technology of firms producing final goods. The aforementioned assumption simplifies the model and captures the reality of the many technological spillovers between industries.

of the form

$$\pi_t(s,r) = \frac{a_t(r)[mc_t(r)\zeta(r,s)]^{-\theta}}{\int_S a_t(v)[mc_t(v)\zeta(v,s)]^{-\theta} dv}. \quad (2.10)$$

And the price index, $P_t(r)$, of a location (where $\Gamma(\cdot)$ denotes the Gamma function) by

$$P_t(r) = \Gamma\left(\frac{-\rho}{(1-\rho)\theta+1}\right)^{-\frac{1-\rho}{\rho}} \left[\int_S a_t(v)[mc_t(v)\zeta(r,v)]^{-\theta} dv\right]^{-1/\theta}. \quad (2.11)$$

Finally, since we are interested in outcomes over long periods of time, we impose trade balance cell by cell. Hence, total income (labor income plus land rents) at r equals total expenditure on goods from r ,

$$w_t(r)L_t(r)H(r) = \int_S \pi_t(v,r)w_t(v)L_t(v)H(v)dv. \quad (2.12)$$

2.4. Climate and the Carbon Cycle

The burning of fossil fuels (as well as other activities, like deforestation) leads to emissions of carbon dioxide into the atmosphere. The carbon cycle defines how carbon flows accumulate in the atmosphere.¹³ The evolution of atmospheric CO₂ follows the dynamics proposed by IPCC (2013) where the stock of carbon in the atmosphere, S_t , evolves according to

$$S_{t+1} = S_{\text{pre-ind}} + \sum_{\ell=1}^{\infty} (1-\delta_{\ell}) (E_{t+1-\ell}^f + E_{t+1-\ell}^x). \quad (2.13)$$

As defined in equation (2.8), E_t^f denotes the endogenous CO₂ emissions from fossil fuel combustion. In addition, E_t^x are exogenous CO₂ emissions from non-fuel combustion, taken from the Representative Concentration Pathways (RCP) 8.5 or 6.0 IPCC scenario. The parameter $S_{\text{pre-ind}}$ denotes the CO₂ stock in the pre-industrial era (1800) and $(1-\delta_{\ell})$ is the share of CO₂ emissions remaining in atmosphere ℓ periods ahead. Higher concentrations of carbon dioxide rise the global radiative forcing, F_{t+1} , (net inflow of energy), which is approximated as in Myhre et al. (1998), so

$$F_{t+1} = \varphi \log_2(S_{t+1}/S_{\text{pre-ind}}) + F_{t+1}^x, \quad (2.14)$$

where φ denotes the forcing sensitivity, that is, the increase in the radiative force when carbon stock doubles with respect to its pre-industrial level. F_t^x denotes the radiative forcing from non-CO₂ greenhouse gases (methane, nitrous oxide, among others), taken from the RCP 8.5 or 6.0 scenarios. When the inflow of energy from the Sun exceeds the outflow of energy exiting the planet, global temperature rises, according to a process

13. Dietz et al. (2021) argues that the dynamics of highly complex general circulation models can be fitted, with a high degree of precision, using reduced-form models, like the one in Joos et al. (2013). This is the carbon cycle model we employ.

defined by

$$T_{t+1} = T_{\text{pre-ind}} + \sum_{\ell=0}^{\infty} \zeta_{\ell} F_{t+1-\ell}, \quad (2.15)$$

where $T_{\text{pre-ind}}$ denotes worldwide temperature over land in the pre-industrial era and ζ_{ℓ} is the current temperature response to an increase in the radiative force ℓ periods ago.

Carbon emissions disseminate in the world quickly and affect global temperature, not local temperatures directly. This is why carbon emissions are a global externality. However, given that we want to quantify our model at a fine geographical resolution, we need to take a stand on the evolution of local temperature in response to changes in global temperatures. We follow [Mitchell \(2003\)](#), who argues that a linear down-scaling relationship provides accurate results.¹⁴ In particular, we let

$$T_t(r) - T_{t-1}(r) = g(r) \cdot (T_t - T_{t-1}), \quad (2.16)$$

where the coefficient $g(r)$ tells us by how much, in °C, temperature in cell r changes when global temperature changes by one °C. The coefficients $g(r)$ depend on local physical characteristics of a location, so we keep them fixed over time.

2.5. *Competitive Equilibrium and Balanced Growth Path*

Together the conditions presented above define a dynamic competitive equilibrium of our model. We can show that the system of equations that defines a spatial equilibrium in a given period can be reduced to a system of equations for population and wages in each location. All other variables, including firm investments, can then be directly computed using the equations presented above.¹⁵ We can show that there exists a unique solution to the system of equations if (i) $\epsilon = 1$ or $v^f = v^c$, and (ii) $\alpha/\theta + \gamma_1/\xi \leq \lambda/\sigma + (1 - \mu) + \Omega/\sigma$. The first condition requires that either the elasticity of substitution between fossil fuels and clean energy is one (Cobb-Douglas) or the innovation elasticity with respect to global real income growth is the same across energy types. Those assumptions allows us to keep the log-linear structure of the model.¹⁶ The second condition generalizes that in [Desmet et al. \(2018\)](#). It states that the static agglomeration economies associated with the local production externalities, α/θ , and the degree of returns to innovation, γ_1/ξ , do not dominate the three congestion forces. These three congestion forces are governed by the value of the negative elasticity of amenities to density adjusted by the elasticity of utility to real income, λ/σ , the share of land in production which determines the degree of local decreasing returns, $1 - \mu$, and the variance of taste shocks adjusted by the elasticity of utility to real income, Ω/σ .

14. More precisely, [Mitchell \(2003\)](#) finds small non-linearities in the local climate response to the length of time over which warming has occurred, to the rate at which it has occurred, and to the extent to which global temperature has stabilized. Incorporating these non-linearities has only a negligible effect on our results.

15. We present detailed proofs in [Supplementary Materials Section I.1](#), but they parallel the reasoning in [Desmet et al. \(2018\)](#).

16. In the model quantification below, our baseline parametrization deviates from this condition slightly, but numerically we find that the solution is robust to a variation in initial conditions.

A spatial equilibrium in a given period determines firm innovation, energy use, and carbon emissions. Then, we use equations (2.1), (2.5), and the climate and carbon cycle model, to determine temperatures and next period’s amenities and productivities. This allows us to compute the dynamic equilibrium forward, period by period, for as many years as needed. As we show in [Supplementary Materials Section I.3](#), eventually the distribution of population across space and the world real output growth rate converge to a Balanced Growth Path (BGP) if: (i) total natality rates $1+n_t(r)$ converge to one as income per capita grows; (ii) the stock of carbon is finite, and $(1-\delta_\ell), \zeta_\ell, E_\ell^x$ and F_ℓ^x converge to constant values, so eventually temperatures stabilize; (iii) $\epsilon=1$ or $v^f=v^c$; and (iv) $\alpha/\theta+\gamma_1/\xi+\gamma_1/(\xi(1-\gamma_2))\leq\lambda/\sigma+(1-\mu)+\Omega/\sigma$. The last condition, which generalizes that in [Desmet et al. \(2018\)](#), states that agglomeration forces, that now include also dynamic agglomeration forces through innovation, $\gamma_1/(\xi(1-\gamma_2))$, are weaker than the three congestion forces. The dynamics of the model are very protracted, so convergence to a Balanced Growth Path is not fully achieved for the four-century horizon that we consider. We now proceed to quantify our model.

3. QUANTIFICATION

We quantify the model at the 1° latitude by 1° longitude spatial resolution, which is the spatial resolution of the G-Econ dataset ([Nordhaus, 2006](#); [Nordhaus and Chen, 2016](#)). Our baseline year is 2000. In order to quantify the model we need values for all the economy-wide parameters, plus location specific values for initial fundamental amenities, productivities, and migration costs, as well as bilateral transport costs. We also need to parameterize the extraction cost of fossil fuels, estimate the damage functions on amenities, productivities, and natality rates, and quantify the carbon cycle and climate module.

We follow the quantification strategy in [Desmet et al. \(2018\)](#) for the common parts of the model. Table 3 in [Online Appendix A](#) summarizes the parameter values used in the baseline case.¹⁷ Local fundamental amenities and productivities are recovered so that the model matches exactly population and income in 2000. Migration costs are recovered so that the model matches exactly the observed change in population between 2000 and 2005. All these local characteristics are exactly identified by an inversion procedure described in detail in [Desmet et al. \(2018\)](#). Bilateral trade costs are based on optimal routing using the fast marching algorithm. In what follows, we describe the estimation of three families of parameters and functions that are new to this paper, namely, the evolution of energy prices; the construction of the damage functions on amenities, productivities, and natality rates; and the carbon cycle, as well as the climate and the down-scaling factors. [Online Appendix A](#) provides details on the data used in the quantification.

3.1. Energy Prices

We split the estimation of the energy component in four steps. First, we parameterize the cost of extracting fossil fuels from the ground, $f(\cdot)$. Second, we calibrate the energy share in production, $\mu(1-\chi)$, and the share of fossil fuels in the energy aggregator, κ .

17. In the baseline quantification we set $\sigma=1$, but perform robustness exercises in [Supplementary Materials Section L.4](#).

Third, we construct prices for fossil fuels and clean energy at the cell level for the year 2000 and use them to estimate the initial level of energy productivities, $\zeta_0^f(\cdot)$ and $\zeta_0^c(\cdot)$. Finally, we set v^f and v^c to match historical data on global CO₂ emissions and clean energy use.

To estimate the cost of extracting fossil fuels $f(\cdot)$, we employ estimates from Rogner (1997) and Bauer et al. (2017). To construct quantity-cost relations for fossil fuel resources, Rogner (1997) analyzed historical marginal production costs for different fossil fuel deposits and found a stable relation across regions and time: extraction costs are flat when resources are abundant, but they rise sharply as the resource gets exhausted.¹⁸ Bauer et al. (2017) extends the work of Rogner (1997) and formulates a database of fossil fuel quantities and extraction costs, taking into account different technological, political and economic conditions. We consider the scenario that closest resembles the most pessimistic scenario (RCP 8.5) of the IPCC (2013).¹⁹ Figure 1 displays, in green, the estimates by Bauer et al. (2017) as a function of cumulative CO₂ emissions. We specify the extraction cost function $f(\cdot)$ as

$$f(CumCO2_t) = \left(\frac{f_1}{f_2 + e^{-f_3(CumCO2_t - f_4)}} \right) + \left(\frac{f_5}{maxCumCO2 - CumCO2_t} \right)^3, \quad (3.17)$$

where $CumCO2_t$ denotes the cumulative CO₂ extracted up to period t and the parameter $maxCumCO2$ denotes the total stock of carbon dioxide available to produce energy on the planet. We consider two values for $maxCumCO2$ depending on the IPCC (2013) scenario (RCP 8.5 or 6.0) that we are trying to match. We set $maxCumCO2$ equal to the cumulative flow of CO₂ for the next five centuries in the corresponding scenario, which amounts to 19,500 GtCO₂ or 9,700 GtCO₂, respectively.²⁰ The rest of the parameters are chosen to fit the estimates of Bauer et al. (2017). The black curve in Figure 1 displays the estimated extraction curve, which is increasing and convex.

We calibrate the parameters χ and κ using the first order conditions of the firm's profit maximization. In particular, since technology is Cobb-Douglas, the world's average relative expenditure in fossil fuels and clean energy, and the ratio of energy expenditures to the wage bill, are constants given by

$$\left(\frac{Q_0^f}{Q_0^c} \right) \left(\frac{E_0^f}{E_0^c} \right)^{\frac{1}{\epsilon}} = \frac{\kappa}{1 - \kappa}, \quad \text{and} \quad \frac{w_0 Q_0 E_0}{w_0 L_0} = \frac{\mu(1 - \chi)}{\mu + \gamma_1 / \xi}. \quad (3.18)$$

18. Drilling costs in the oil and gas industry increase drastically with depth and coal mining is highly sensitive to the characteristics of deep-lying coal seams.

19. Specifically, Bauer et al. (2017) presents estimates for five Shared Socioeconomic Pathways (SSP), which consider different assumptions for the evolution of the world economy. We choose the scenario SSP5 (development based on fossil fuels), which is the one closest to RCP 8.5, and aggregate the costs of coal, natural gas, and oil into a single fossil fuel in terms of tCO₂ per usd.

20. In comparison, Bauer et al. (2017) considers a total stock of carbon dioxide of 12,550 GtCO₂ and Mcglade and Ekins (2015) of 14,666 GtCO₂. Supplementary Materials Section L.3 presents results for a variety of alternative values for the total stock of carbon.

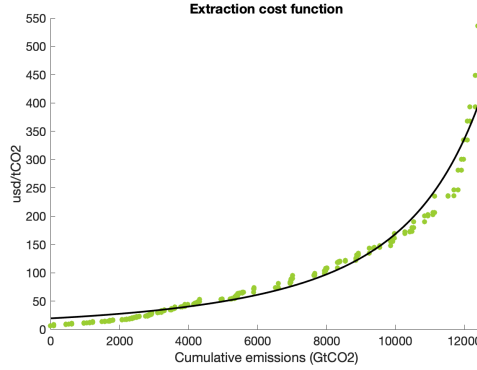


FIGURE 1

The extraction cost function $f(\cdot)$.

We take the elasticity of substitution ϵ from [Popp \(2004\)](#),²¹ who consider a value of 1.6 and obtain global income from the G-Econ database, so $w_0 L_0 = 46.59$ trillions usd for the year 2000. We construct the global price of fossil fuels by aggregating the price of coal, natural gas, and oil as in [Goloso et al. \(2014\)](#).²² This procedure yields an estimate for the price of fossil fuels of $w_0 Q_0^f = 72.99$ usd/tCO₂. [Acemoglu et al. \(2020\)](#) estimates the price of clean energy to be 1.15 times that of natural gas. We use that relation to obtain a price of 87.79 usd per ton of oil equivalent (toe). In turn, one ton of oil equivalent generates 2.8466 tons of CO₂, which is the weighted average of carbon intensities of coal, oil, and natural gas for the year 2000. With those prices and considering that the use of energy from fossil fuels is $E_0^f = 8.88$ Gtoe ([IPCC, 2013](#)) and from clean sources is $E_0^c = 1.23$ Gtoe ([BP, 2019](#)) we obtain $\kappa = 0.89$ and $\chi = 0.96$.²³

The next step is to measure the productivity of fossil fuels, $\zeta_0^f(\cdot)$, and clean energy, $\zeta_0^c(\cdot)$, in the initial period for each cell. To do so, we use the first order conditions of the firm's optimization problem in each cell, together with equation (2.7), to obtain

$$\zeta_0^f(r) = \left(\frac{\mu + \gamma_1 / \xi}{\mu(1 - \chi)\kappa} \right) \left(\frac{e_0(r)}{L_0(r)} \right) \left(\frac{e_0^f(r)}{e_0(r)} \right)^{\frac{1}{\epsilon}} f(\text{CumCO}_2), \quad (3.19)$$

21. [Papageorgiou et al. \(2017\)](#) finds that the elasticity of substitution for electricity generating industries is 2 and for non-energy industries is 3. Sensitivity analysis to this parameter are conducted in Section 4.4 and [Supplementary Materials Section L.2](#).

22. [Goloso et al. \(2014\)](#) proposes that energy from fossil fuels is a CES composite of coal, natural gas, and oil, with elasticity of substitution of 1.11, which corresponds to the unweighted average of the elasticity of substitution between coal and oil, coal and natural gas, and oil and natural gas, according to [Stern \(2012\)](#). [Acemoglu et al. \(2020\)](#) focuses on the electricity sector and consider an elasticity of substitution of 2, in line with [Bosetti et al. \(2007\)](#), so that fossil fuels are more substitutable between them than with respect to clean energy. The representative prices of oil, natural gas and coal are the average of the Brent, U.S. Henry Hub, and U.S. Central Appalachian, respectively, over the period 1983-2017 to smooth short-run fluctuations. Data on prices is taken from [BP \(2019\)](#) and data on quantities from [IEA \(2019\)](#).

23. This parametrization implies that the energy share in production is 3.3%, which is slightly smaller than the values used in the literature, where [Goloso et al. \(2014\)](#) uses 4%, [Hassler et al. \(2019\)](#) 5.55% and [Krusell and Smith \(2022\)](#) 6%.

$$\zeta_0^c(r) = \left(\frac{\mu + \gamma_1/\xi}{\mu(1-\chi)(1-\kappa)} \right) \left(\frac{e_0(r)}{L_0(r)} \right) \left(\frac{e_0^c(r)}{e_0(r)} \right)^{\frac{1}{\varepsilon}}. \quad (3.20)$$

Labor at the cell-level is directly taken from the G-Econ database. To construct cell-level energy use of fossil fuels and clean energy, we first start with data for CO₂ emissions and clean energy use at the country-level from BP (2019), Crippa et al. (2019) and IEA (2019). Then, we allocate energy use across cells within countries using the share of emissions in the Emissions Database for Global Atmospheric Research (EDGAR, Crippa et al., 2019).

Finally, to estimate the elasticity of technology in the fossil fuel sector, v^f , and in the clean energy sector, v^c , with respect to global real GDP growth, we construct historical global CO₂ emissions and clean energy use from IEA (2019) and BP (2019). We then run the model backwards in time for 50 periods and find the elasticities that provide the best fit of the historical data on relative energy use. The resulting elasticity for clean energy is larger than the one for fossil fuels since its use has expanded faster over time ($v^c = 1.22 > 1.16 = v^f$).²⁴

3.2. The Effect of Local Temperature on Amenities and Productivities

To estimate the damage functions $\Lambda^a(\cdot)$ and $\Lambda^b(\cdot)$, which determine how temperature affects the fundamentals of the economy, we first need to compute fundamental amenities and productivity in each location by *inverting the model*. The inversion of the model requires solving the equilibrium system of equations for $\bar{b}_t(r)$ and $\bar{a}_t(r)$ using data on wages and population, as well as the data on the amount of land in each cell, and the energy prices we described in the previous section. We can do so for the four periods of data available in G-Econ, namely, 1990, 1995, 2000 and 2005.²⁵

The model inversion exactly identifies $\bar{a}_t(r)$ and $\bar{b}_t(r)/u_t(r)$, but is unable to separate $\bar{b}_t(r)$ apart from $u_t(r)$. Intuitively, we cannot identify the numerator from the denominator since, if we observe many individuals in a poor location, it could be because amenities are high or because individuals are trapped there even though utility is very low. To disentangle a location's amenities from its initial utility, we require a measure of utility.²⁶ Desmet et al. (2018) uses as utility measure a subjective well-being survey from the Gallup World Poll. However, this data is only available for one period and only at the country-, rather than cell-level. Thus, we use the Human Development Index (HDI) as our measure of $u_t(r)$ after transforming it into a cardinal measure of well-being that is linear in log-real income, as in our model.²⁷

Once we compute the fundamentals that rationalize the observable data on wages, population, and energy prices, we identify the causal effect of temperature on amenities and productivities using a panel fixed-effects empirical specification, with temperature

24. Supplementary Materials Section I.4 outlines the system of equations that solve the model backwards in time and Online Appendix C describes, in further detail, the estimation of these elasticities.

25. Supplementary Materials Section I.2 describes the inversion of the model in more detail. An alternative approach that would give us a longer time series would be to employ data on production from Kummu et al. (2018). This dataset spans a longer period of time, from 1990 to 2015 at a yearly frequency, but it displays a coarser geographical resolution with around 700 sub-national units.

26. Once we identify $\bar{b}_t(r)$, we can obtain the migration costs in order to match the model-implied net migration flows with the ones observed in the data

27. Supplementary Materials Section I.2 describes the details of this calculation and compares this index to the measure used in Desmet et al. (2018).

entering the regression in a flexible non-parametric way. Our main empirical specification is given by

$$\begin{aligned} \log(x_t(r)) = & \sum_{j=1}^J \delta_j^x \cdot T_t(r) \cdot \mathbb{1}\{T_t(r) \in \mathcal{T}_j\} + \delta^z \cdot Z(r) \cdot \mathbb{1}\{x_t(r) = \bar{a}_t(r)/\phi_t(r)\} \\ & + \iota(g) \cdot \mathbb{1}\{x_t(r) = \bar{b}_t(r)\} + \iota_t(s_x) + \varepsilon_t(r) \end{aligned} \quad (3.21)$$

where $x_t(r) \in \{\bar{b}_t(r), \bar{a}_t(r)/\phi_t(r)\}$ are the fundamental amenities and the ratio of fundamental productivities to innovations at cell r in period t . We use the ratio $\bar{a}_t(r)/\phi_t(r)$ in order to account for the effect of endogenous innovation on fundamental productivity over time. The variable $T_t(r)$ denotes the average January temperature for locations in the Northern Hemisphere and the average July temperature for locations in the Southern Hemisphere over the last decade. The variable $\mathbb{1}\{T_t(r) \in \mathcal{T}_j\}$ is an indicator function of temperature $T_t(r)$ being in interval \mathcal{T}_j . We partition the distribution of temperatures into $J = 20$ bins, each comprising 5% of the observed temperature values.²⁸ Average January or July temperatures over land, respectively, range from -50.15°C to 32.85°C .

The non-parametric specification in (3.21) accommodates the potential non-linearities and bliss-points in the effect of temperature on these fundamentals. That is, a temperature increase of 1°C might have different impacts in very cold regions, like Siberia, with respect to very hot places, like the Sahara. Thus, the coefficient of interest δ_j^x , which is the semi-elasticity of $x_t(r)$ with respect to temperature, is allowed to vary according to the level of temperature. This implies that the damage function $\Lambda^x(\cdot)$ can be expressed as the semi-elasticity δ_j^x , evaluated at the current level of temperature, times the change in local temperature, namely, $\Lambda^x(\Delta T_t(r), T_{t-1}) = \delta^x(T_t(r)) \cdot \Delta T_t(r)$.

Our specification also incorporates a set of time-invariant controls at the cell level, $Z(r)$, fixed-effects, $\iota(g)$, and regional time trends, $\iota_t(s_x)$, to alleviate potential omitted variable bias.²⁹ To the extent that temperature is spatially correlated, any variable not included in the estimation, that is spatially correlated, would appear in the error term and would bias our estimate of the coefficient δ_j^x . To estimate the effect of temperature on productivity, we follow Nordhaus (2006) and include a number of geographic attributes as cell-level covariates, $Z(r)$.³⁰ We also include time-varying sub-national fixed-effects, $\iota_t(s_x)$, that divide Europe into four regions. Geographic attributes have a direct impact

28. We employ decadal rather than yearly temperature to capture the long-run effects of temperature thereby exploiting also cross-sectional variation. We employ January and July, rather than yearly temperatures, because the former exhibits larger variation over space, which allows us to better identify the temperature impact on fundamentals. January and July temperatures are also correlated with temperature variability which allows us to capture some of the effects of changes in extreme weather patterns as temperatures change (see [Online Appendix B.2](#)). We perform robustness exercises in [Supplementary Materials Section M.2](#), where we present results for average temperatures. Consistent with this argument, the results show larger gains in colder regions and smaller in warm ones. The point estimates are noisier too.

29. We use two definitions of sub-national units. We start with the administrative units defined in [Kummu et al. \(2018\)](#) for the whole world and aggregate those in Europe at the (i) country level and (ii) at the region level: North, South, West and East of Europe.

30. We specify $Z(r)$ as an additive separable Chebyshev polynomial of order 5 in mean and standard deviation of elevation, roughness, distance to the coast, distance to the ocean, and distance to a water body, as well as a fixed-effect for land type.

on local productivities in agriculture, but also in other sectors through the availability of raw materials and transportation networks. Broader regional evolution in technology depends on regional specialization rather than national boundaries and so is captured through the many sub-national trends in the world and the four European regions. To estimate the effect of temperature on amenities, we use fixed effects for a partition of the gridded map into blocks of size 2 cells by 2 cells, denoted by $\iota(g)$. Although slightly more spatially aggregated, this specification captures any time-invariant local characteristic at the 2-cell spatial level. We also include sub-national fixed-effects, $\iota_t(s_x)$. Amenities are driven by many local characteristics that are hard to explicitly control for, as well as by differences in national history and culture. Hence, using a flexible set of fixed effects and trends is important.³¹

Our estimation of both damage functions exploits observations for more than 17,000 locations over four periods of time. The large heterogeneity in temperature at the worldwide level allows us to estimate the effect of temperature on fundamental amenities and productivities as a function of local temperature levels, explicitly controlling for migration, trade, and innovation as long-run adaptation mechanisms. By controlling for local characteristics or block fixed effects, as well as sub-national trends, we obtain causal estimates of warming damages. In this sense, our empirical strategy can be classified as a new approach within the *Climate Adaptive Response* estimation literature (Auffhammer, 2018).

Figure 2 displays the baseline estimates of $\delta^b(T_t(r))$ and $\delta^a(T_t(r))$. We allow for spatially correlated errors as in Conley (1999).³² The bars in the figure denote the point estimates, the whiskers the 95% confidence intervals, and the solid gray curve a logistic approximation.³³ The dashed gray lines represent the 95% confidence intervals of the logistic curves.³⁴

As expected, for very cold regions, increases in temperature raise both amenities and productivities. For example, in the coldest bin of January-July temperatures, centered at -37.79°C , an increase in 1°C augments local amenities by 2.16% and local productivities by 7.44%, according to the logistic smoothing. In bins with warmer temperatures, the beneficial effects of rising temperatures decline, until they reach zero and eventually turn negative. For January-July temperatures in the warmest bin, centered at 25.77°C , an increase in 1°C reduces local amenities by 2.24% and local productivities by 16.57%. These results highlight the heterogeneous effects of temperature on fundamentals across the range of temperature levels experienced in regions of the world. Extreme temperatures have negative effects on amenities and productivities. Bliss-points, the optimal temperatures for fundamentals, are given by the moderate temperatures at which

31. Online Appendix B.1 describes the details of the damage function estimation, Supplementary Materials Section M.2 presents a number of robustness exercises and considers different structures for the error term

32. We consider that the correlation of errors between cells declines linearly with distance, so that when distance is greater than 550 km (5 cells), correlation vanishes to zero.

33. We opted for a logistic approximation to be conservative when extrapolating damages to temperatures that are hotter than the ones historically observed. Albouy et al. (2016) and Graff-Zivin and Neidell (2014) argue that individuals reduce their time outdoors as temperatures become uncomfortable, reducing their sensitivity to further temperature changes.

34. The upper (lower) confidence interval of the logistic curve is constructed using the upper (lower) confidence interval of the point estimates and fitting a logistic curve as well.

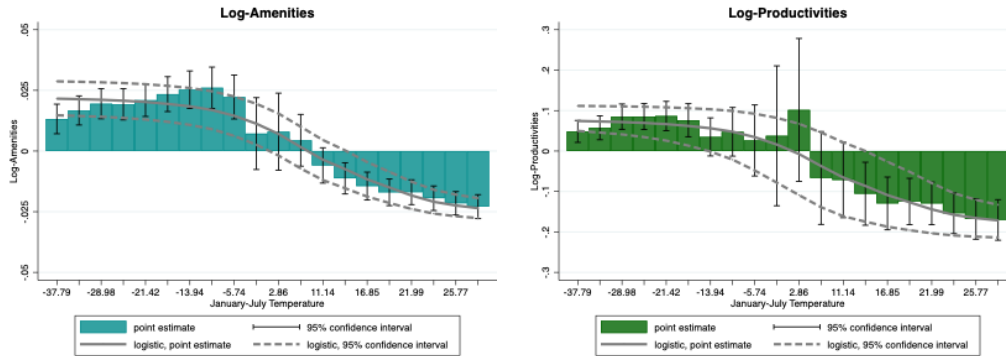


FIGURE 2

Effect of temperature on fundamental amenities and productivities, using January temperatures for the Northern Hemisphere and July temperatures for the Southern Hemisphere.

$\delta x_j = \frac{\partial \log(x_t(r))}{\partial T_t(r)}$ equals zero. For amenities we estimate an optimal winter temperature of 8.6°C , whereas for productivities of 1.6°C .³⁵

The damage functions estimated above capture the impact of changes in the winter's average temperature on the fundamentals of the economy. Higher concentrations of greenhouse gases have been associated not only with average temperatures but also with the dispersion of temperatures throughout the year. In [Online Appendix B.2](#), we extend the damage functions to incorporate different measures of temperature variability. Because first and second moments are correlated, we find that the baseline empirical specification is not affected significantly. Changes in extreme temperatures are already effectively captured by our main specification. Another potential concern with our specification of damage functions is that it features only an aggregate sector. Of course, locations vary dramatically in their sectoral composition. In [Online Appendix B.3](#), we incorporate the role of heterogeneity across economic sectors by allowing the damage function to vary according to the share of value added in agriculture. Our results show that areas specializing more in agriculture are more climate-sensitive for both amenities and productivities. When simulating the model with damage functions that depend on the agricultural share (which we keep fixed), we find a similar spatial pattern for the impact of climate change. Overall, we find welfare losses 1 percentage point lower than in our baseline scenario, since many locations intensive in agriculture lie in cold parts of the world.

35. Although the literature has not estimated the impact of temperature on fundamentals, rather than endogenous outcomes, our estimates are roughly in line with available studies. [Burke et al. \(2015b\)](#) employs country-level data for the period 1960-2010 and, through panel methods, estimate that economic production is concave in annual temperature peaking at 13°C . [Krusell and Smith \(2022\)](#) considers that a yearly temperature of 11.6°C maximizes productivity and [Nordhaus \(2006\)](#) estimates that the optimal yearly temperature for output lies between 7°C and 14°C . If we translate this range to January-July temperatures, which is the temperature measure we use in our estimation, this range becomes -5°C to 6°C , which includes our bliss-point for productivity. To further frame our empirical specification relative to standard methods, in [Supplementary Materials Section M.3](#) we also perform a naive estimation of the damage functions in equation (3.21) using population density, wages, and real GDP at the cell-level as outcomes. We obtain results that are consistent with the findings in the literature, although they fail to incorporate long-run adaptation mechanisms.

3.3. The Effect of Income and Temperature on Natality Rates

We specify local natality rates as a function of real income and temperature. In particular, we let $n_t(r) = \eta^y(\log(y_t(r))) + \eta^T(T_t(r), \log(y_t^w))$, where

$$\begin{aligned} \eta^y(\log(y_t(r))) &= \mathcal{B}(\log(y_t(r)); b^\ell) \cdot \mathbb{1}(\log(y_t(r)) < b^*) \\ &\quad + \mathcal{B}(\log(y_t(r)); b^h) \cdot \mathbb{1}(\log(y_t(r)) \geq b^*), \end{aligned} \quad (3.22)$$

$$\eta^T(T_t(r), \log(y_t^w)) = \frac{\mathcal{B}(T_t(r); b^T)}{1 + e^{b_w[\log(y_t^w) - \log(y_0^w)]}}, \quad (3.23)$$

with $\mathcal{B}(\log(y_t(r)); b) = b_0 + b_2 e^{-b_1[\log(y_t(r)) - b^*]^2}$. The term $\eta^y(\cdot)$ captures the standard argument in [Becker \(1960\)](#) that, as income grows, household substitutes quantity for quality by investing more in their children. [Delventhal et al. \(2021\)](#) analyzes birth and death rates across countries and find that almost all countries in the world have experienced (or are experiencing) a demographic transition, that is, they move from a phase of high to one of low natality. Furthermore, they argue that the start of this transition occurs at roughly the same income level. Hence, the functional form in (3.22) specifies an inverse and asymmetric bell-shaped function, so that when income is sufficiently low, natality rates are high but, as income grows, natality rates decline until they reach negative values, as evidenced by some rich countries today. To impose that global population is stable in the very long-run, natality rates tend towards zero as income rises further.³⁶

The relation between temperature and natality is captured by $\eta^T(\cdot)$. [Carleton et al. \(2022\)](#) estimates that higher income allows households to adapt to changes in temperature, thereby flattening the mortality response to temperature. [Barreca et al. \(2016\)](#) argues that access to health care, electricity and, particularly, air conditioner have been important adaptation mechanisms. Thus, we specify $\eta^T(\cdot)$ as a symmetric bell-shaped function, so that when temperatures are extreme, natality rates are low, and they are maximized in temperate climates. Finally, we interact this component with a decreasing function of global income, y_t^w , to account for the remedies that a wealthier world would provide for the effect of temperature on mortality.

To estimate the parameters defining the natality rate function, b^ℓ, b^h, b^T, b_w , we run the model backward for 50 periods and compute the endogenous historical population levels predicted by the model. We then find the coefficients that maximize the model's fit with the country-level historical data on natality rates ([UN, 2019](#)).³⁷ Figure 3 displays the resulting functions $\eta^y(\cdot)$ and $\eta^T(\cdot)$.³⁸ They illustrate the position of the world average,

36. $\mathcal{B}(\cdot)$ is a bell-shaped function where b_0 and $b_2 + b_0$ are the minimum and maximum (maximum and minimum) values if $b_2 > 0$ ($b_2 < 0$), $b_1 > 0$ governs the slope of the incline and decline, and b^* is the value that maximizes the function.

37. We weight countries by population size with additional weight given to more recent observations. Additionally, we impose that the natality function $\eta(\cdot)$ matches the global natality rate in 2000 and 2020. Figures 56 and 57 in the [Online Appendix](#) compare the historical global natality rates from the data and the estimation and the cross-section of country-level natality rates in 2000, respectively.

38. The left panel of Figure 3 suggests that tropical zones, that will experience negative income impacts from global warming, will experience higher natality rates. The opposite is expected to happen in arctic zones. These findings are in line with [Casey et al. \(2019\)](#), which rationalizes a range of economic channels driving these spatial patterns, like sectoral reallocation, gender gaps, longevity, and child mortality.

a cold and rich country (United States), and a hot and poor country (Zambia), for the years 1950 and 1999.

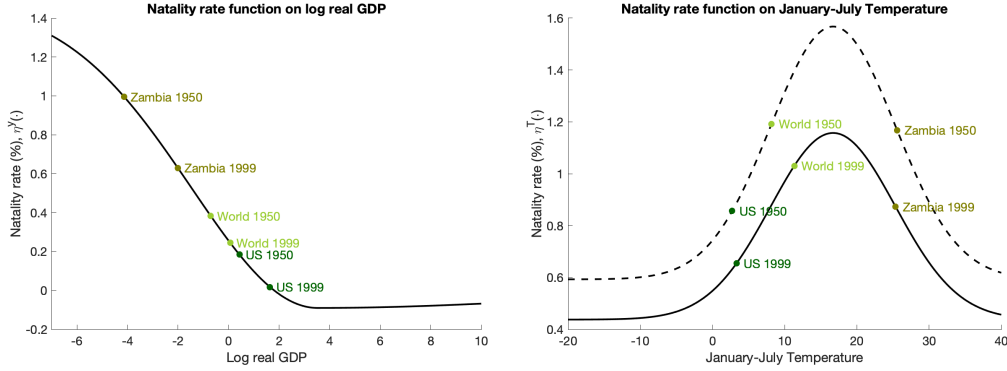


FIGURE 3
The natality rate function.

Finally, with the quantified natality rate function, we compute the migration costs $m_2(\cdot)$ that make the model exactly rationalize the population levels observed in 2005. The procedure to obtain the migration costs is described in detail in [Supplementary Materials Section I.5](#) and the procedure to estimate the natality function, as well as some additional related results, are presented in [Online Appendix C](#).

3.4. Carbon Cycle and Temperature Down-scaling

We adopt the specification of the carbon cycle and the global climate component proposed by [IPCC \(2013\)](#). We choose parameter values such that the carbon cycle in [Section 2.4](#) exactly reproduces the values displayed in [IPCC \(2013\)](#). The details and exact values used are discussed in [Online Appendix D](#). As we will show below, the end result will be that the endogenous evolution of temperature in our baseline scenario will reproduce the temperature paths of the RCP 8.5 or 6.0 scenarios almost exactly.

We use equation (2.16) to down-scale worldwide temperature at the cell level. We use the Berkeley Earth Surface Temperature Database ([Rohde and Hausfather, 2020](#)), which provides temperature data at a geographic resolution of $1^\circ \times 1^\circ$. In order to obtain a smooth spatial shape of the temperature scaler, $g(\cdot)$, we specify it as a function of the geographical attributes of each cell. Specifically, as a Chebyshev polynomial of order 10 on latitude and longitude (including a cross term), elevation, distance to the coast, distance to non-frozen oceans, distance to water bodies, vegetation density, the share of ice-covered land, and albedo.³⁹ We estimate equation (2.16) by weighted OLS, with higher weight given to more recent observations. The estimation procedure yields a good fit; it captures 83% of the variation in the local temperature data. [Online Appendix D](#) elaborates further on the construction of the temperature scaler.

Figure 4 plots the local January-July temperatures in 2000 and the temperature scaler for every cell of the world. An increase in global temperature of 1°C results in increases

39. Albedo is the ratio of light that a surface reflects compared to the total sunlight it receives. Surfaces that reflect a lot of light are bright and have a high albedo. For example, snow has a high albedo, whereas forests have a low albedo.

as large as 2.2°C close to the north pole, but as low as 0.5°C in southern locations in Central and South America, Africa, South East Asia, and Australia. Coastal regions tend to experience smaller increases in temperature compared to inland locations. This pattern is attributed to the fact that land absorbs more heat than water. These results are in line with predictions by IPCC (2007). Overall, Figure 4 illustrates the large heterogeneity in the impact of global warming on local temperatures and underscores the importance of a high-resolution spatial model.

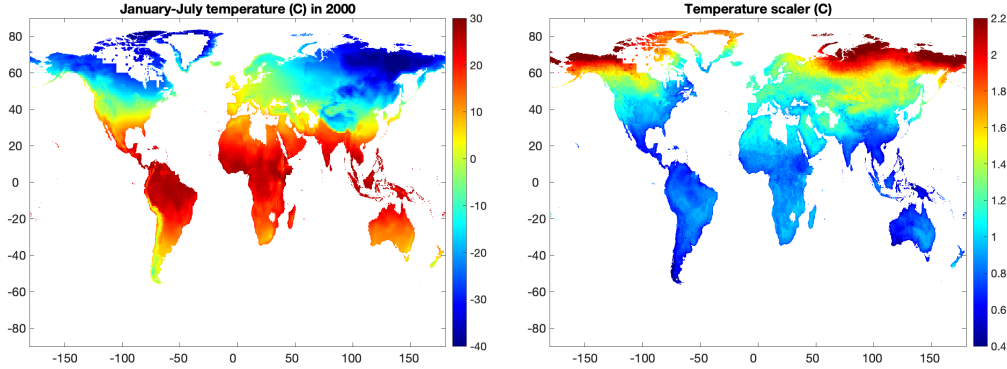


FIGURE 4
Local January-July temperature in 2000 and temperature scaler.

4. THE BASELINE SCENARIO

In the baseline scenario, we consider the two quantifications based on the RCP 8.5 and 6.0 carbon cycle calibrations.⁴⁰ We obtain predictions for 400 years, corresponding to the period 2001 to 2400. These scenarios assume that no new climate policy is put in place and that the evolution of clean technology follows the process described in the previous sections. We organize the exposition of the quantitative results as follows. First, we describe the endogenous evolution of aggregate CO₂ emissions and average global temperature and compare them with the projections by IPCC (2013). Then, we explore the corresponding evolution of economic outcomes, namely, amenities, productivities and population density. Finally, we run counterfactuals where we eliminate the effect of the rise in temperatures in order to evaluate the welfare effects of global warming.

4.1. Emissions and Temperature in the Baseline Scenario

Figure 5 presents the paths for CO₂ emissions predicted by the model, as well as their comparison with the corresponding projections in IPCC (2013). Carbon dioxide emissions from fossil fuel combustion are expected to grow over the current century, since economic growth and the resulting improvements in fossil fuel technology overcome the increase in the relative price of carbon-based energy that results from the larger extraction cost associated with increasing cumulative emissions. For the carbon cycle calibration based

40. As described above, each of these calibrations determines the size of fossil fuel deposits, $maxCumCO_2$; the flow of CO₂ emissions from land use, E_t^x ; and the flow of non-CO₂ greenhouse gases, F_t^x .

on the RCP 8.5 (6.0) scenario, CO₂ emissions reach a peak of 117 GtCO₂ (49 GtCO₂) in 2110 (2079), a value slightly higher (lower) than the 106 GtCO₂ (63 GtCO₂) of the IPCC scenario. After those points, the flow of carbon dioxide declines towards zero, since extraction costs increase sharply as fossil fuels become exhausted. Note that, although the bell-shaped carbon dioxide emission path is an endogenous outcome, derived from the optimizing behavior of agents, it parallels the exogenous abatement process that makes the emission projections of IPCC (2013) decline eventually.

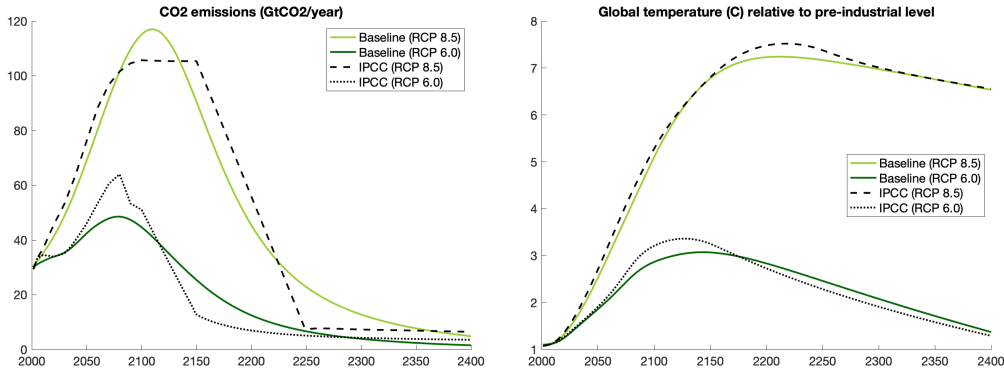


FIGURE 5

CO₂ emissions and global temperature.

The rise in the concentration of greenhouse gases increases global temperatures, as shown in Figure 5, so that by the end of the current century, global temperature is expected to rise 5.1°C (2.9°C) with respect to its pre-industrial level in the RCP 8.5 (6.0) quantification. By 2200, the rise in global temperatures reaches 7.2°C (2.8°C). As carbon dioxide consumption declines towards zero, global temperature approximates its long-run level at between 6°C and 7°C (1°C and 2°C) above pre-industrial level. As expected, given our parametrization of the carbon cycle and the close match between the emissions trajectories in our model and those in the RCP 8.5 or 6.0 scenarios, the temperature evolution matches the IPCC scenarios almost exactly.

As illustrated in Figure 4, the increase in global temperatures yields heterogeneous increases in local temperatures across the world. In 2000, only 26.97% of the land surface experienced January-July temperatures higher than 20°C. In the RCP 8.5 (6.0) quantification, two hundred years later this share is predicted to increase to 40.80% (30.81%), covering most of North and Central Africa, the Middle East, India, Brazil and Central America. At the other extreme, in 2000, 5.50% of the global land surface exhibited January-July temperatures below -30°C, mainly located in North Canada, Greenland, and Northern Russia. This share is expected to decline to 0.30% (3.68%) in 2200.

4.2. Local Amenities, Productivity, and Population in the Baseline Scenario

To measure how changes in temperature distort economic outcomes, we compare two scenarios: A factual scenario, our baseline, in which temperature affects fundamental amenities, productivities, and natality rates as described in Section 3, and a counterfactual scenario, in which temperature does not disrupt these fundamentals and, therefore, has no effect on economic outcomes.

Figure 6 shows the ratio of fundamental amenities and productivities in 2200 in the scenario with global warming relative to the counterfactual scenario without global warming in the RCP 8.5 quantification.⁴¹ Values greater (lower) than one indicate that temperature changes are predicted to increase (decrease) the respective fundamental characteristic. As we argued before, the estimated temperature damage functions, $\Lambda^b(\cdot)$ and $\Lambda^a(\cdot)$, imply that rises in temperature have heterogeneous effects over space depending on the level of temperature. In the RCP 8.5 (6.0) quantification, in the year 2200 the coldest places in the world experience amenity gains as large as 38% (10%), while the hottest places in the world are projected to suffer amenity losses of 25% (7%). The pattern of changes in amenities depends primarily on latitude, with equatorial regions losing the most, but the geographic patterns are quite rich. Inland regions in Africa, South America, and Australia lose more than what their latitude would predict, as does the U.K., and parts of continental Europe. The average amenity losses, weighted by the 2200 population in the baseline scenario, amount to 4.9% (1.3%).

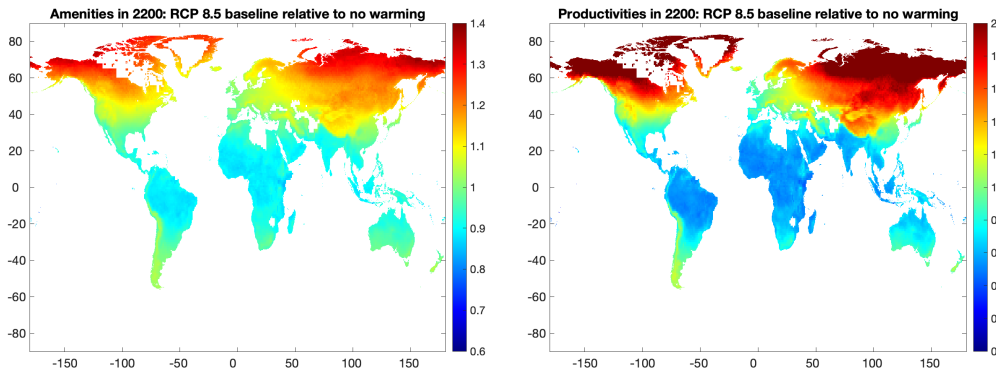


FIGURE 6

Gains and losses in amenities and productivities from global warming in the year 2200.

The impact of global warming on fundamental productivities by 2200 exhibits similar patterns, although more pronounced. Note that the effects on productivity are not only driven by the direct impact of temperature on the estimated damage function, $\Lambda^a(\cdot)$, but also by endogenous innovation decisions. In parts of Alaska, Northern Canada, Greenland, and Northern Russia productivity doubles relative to the scenario without global warming, and in a few areas the changes in productivity can be even larger. In contrast, in Brazil, Africa, the Middle East, India, and Australia we observe declines in productivity of up to 80% (30%), in the RCP 8.5 (6.0) quantification. On average, and again weighting by population in the baseline scenario, world fundamental productivity declines by 25% (5%) by 2200 due to rising temperatures

The geographic configuration of amenities and productivities determines the desirability for residing and producing in particular regions of the world. As the world becomes warmer, the regions where amenities and productivity deteriorate see their population decline. The magnitude of the decline depends on natality rates and migration costs, as well as their trade network and other local characteristics. Figure 7 presents population

41. [Online Appendix E](#) presents symmetric results for amenities, productivity, and population in the RCP 6.0 scenario. Those results show that the regional distribution of changes is very similar, although magnitudes are naturally smaller.

density in 2200 in the RCP 8.5 quantification relative to the counterfactual scenario without global warming. Clearly, global warming generates migration towards colder places. Areas to the south of the 30° latitude in the Northern Hemisphere tend to lose population, while areas to the north tend to gain. Most of the developed world (U.S., Europe, and Japan) is just at the boundary and so is not greatly affected. In two centuries, population density in the north of the world is projected to increase by more than 83% (18%), whereas locations close to the Equator are projected to experience declines in population density as large as 32% (9%), in the RCP 8.5 (6.0) quantification. Note that, although inflow migration to the coldest regions is large in relative terms, it is small in absolute terms, since these areas are only sparsely populated. Overall, the RCP 8.5 (6.0) quantification indicates that by 2200, 4.4% (1.2%) of the population resides in a different location due to global warming. More than 483 (132) million people are displaced by this dimension of climate change, namely global warming, alone!

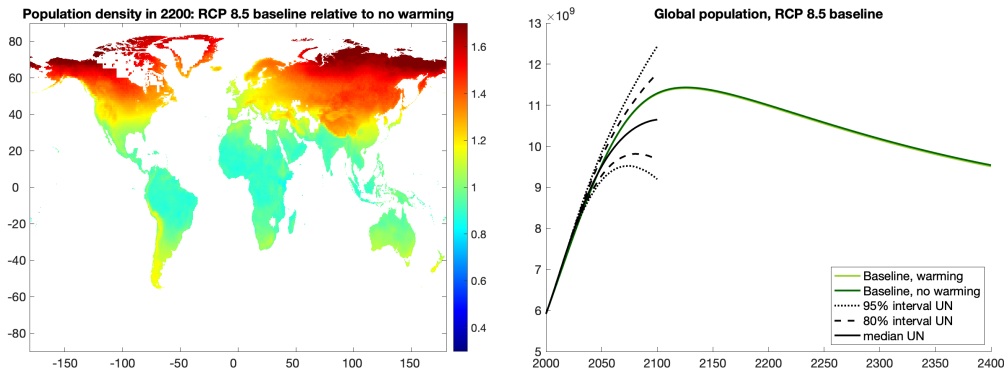


FIGURE 7

Spatial pattern of population and global population.

Global warming not only affects relocation of population across space but also its global level. In the RCP 8.5 (6.0) quantification, the world population grows until the year 2125 (2123), reaching a peak of 11.4 (11.4) billion inhabitants, as depicted in Figure 7. Afterward, population declines as the world gets richer and natality rates decline. Since natality rates converge to zero as income grows, global population converges to a stable long-run level. The figure also presents the United Nations global population estimates. The model's population predictions for the first century are somewhat higher than the median estimate by UN (2019), but within the 80% confidence interval. The long-run level of global population estimated by UN (2004) at 9 billion inhabitants is close to our projection in 2400. Global warming has a relatively small impact on world population, the RCP 8.5 (6.0) quantification predicts that higher temperatures lower population in the next 50 years by roughly 4 (2) millions; in the next 100 years by 16 (8) millions; and in the next 200 years by 27 (10) millions.⁴²

42. The finding that climate change does not affect total populations by much, does not imply that incorporating endogenous natality rates into our spatial assessment model is superfluous, since natality rates affect the baseline economy impacted by climate change. [Supplementary Materials Section L.5](#) gauges the overall impact of endogenizing natality rates and shows that welfare losses in a world with a fixed population are about 1% lower in the RCP 8.5 quantification.

4.3. *The Welfare Cost of Global Warming*

To evaluate the welfare consequences of global warming, we compute the present discounted value (PDV) of local utility that is not idiosyncratic, namely, $\sum_{t=0}^{\infty} \beta^t u_t(r)$.⁴³ We use a value of the discount factor of $\beta=0.965$.⁴⁴ Our choice of the discount factor is restricted by a real output growth rate that is slightly larger than 3% per year. Clearly, to do proper comparisons we need a discount factor for which present discounted values remain finite in all exercises.

Figure 8 displays the spatial distribution of welfare effects, as well as an initial population weighted histogram of the distribution of gains and losses for the RCP 8.5 (top panels) and 6.0 (bottom panels) quantifications.⁴⁵ As before, values smaller than one indicate that the region suffers losses from global warming. The welfare effects of this phenomenon are quite heterogeneous across space. The RCP 8.5 (6.0) quantification indicates that welfare losses range from 20% (4%) in Central and Southern Africa to gains of 11% (4%) in the most northern parts of Russia.⁴⁶ The right-hand panels of Figure 8 clearly show that the distribution of damages is bi-modal. The left peak of the distribution, with losses of around 10% (1%), corresponds to India, while the right peak, which experiences small effects, corresponds to parts of China, Europe, Japan, and the U.S. On average, the world is expected to experience welfare losses of 6% (1%).⁴⁷ The comparison of the results for the two RCP quantifications reveals that the spatial patterns are mostly preserved, although the magnitudes are naturally smaller in the less severe RCP 6.0 quantification.

Figure 9 presents, for both RCP quantifications, scatter-plots of the local welfare losses from global warming versus local real GDP per capita in year 2000. The colors indicate different areas of the world, and the size of each dot represents the population

43. Our specification of welfare considers the discounted utility of agents alive in the initial period. However, since population is endogenous in our model, we could modify our measure of welfare to incorporate also the utility of offsprings. Specifically, we can define local welfare as $\sum_{t=0}^{\infty} \beta^t (1 + \varrho \cdot n_t(r)) u_t(r)$, where $n_t(r)$ denotes the local natality rates in period t and $\varrho \in [0, 1]$ controls the weight given to offsprings. When $\varrho=0$, we are in the baseline case. Rising ϱ from zero to one has only a minuscule effect on global welfare losses (they are 0.013 percentage points smaller), with negligible effects also on their spatial distribution (the largest differences are around 0.03 percentage points). Hence, we restrict attention to the case with $\varrho=0$.

44. The effective discount factor over the long-run is given by $\beta(1+g_c)^\sigma$, where g_c is the BGP growth rate of consumption. g_c is constant over space but depends on the distribution of economic activity across locations which is impacted by global warming. Note the similarities with the climate literature (e.g., Nordhaus, 2017; Golosov et al., 2014), which uses the Ramsey formula. In [Supplementary Materials Section L.1](#) we present robustness exercises with respect to the discount factor.

45. Global average welfare losses are calculated as the population weighted average of the relative present discounted value of utility in the baseline case relative to the counterfactual without global warming.

46. Inevitably, our model abstracts from an array of climate phenomena that might disturb economic performance in the northern latitudes, like permafrost melting, shoreline vulnerability, disease vector emergence, wildfires, among others ([USGCRP, 2018](#)). Consequently, our estimates might overestimate the warming benefits in cold regions.

47. [Supplementary Materials Sections J.1 and J.2](#) present the losses in the present discounted value of real GDP. The spatial distribution and shape of the histogram are similar to those for welfare. However, the largest losses, 10% (2%), largest gains, 3% (1%), and standard deviation, 0.02 (0.004) are smaller than those for welfare. This is natural since the welfare calculation includes the effect of temperature on amenities which intensifies the magnitude and dispersion of climate damages around the world. Furthermore, as we showed in [Figure 7](#), global warming makes people move to locations that have, at least initially, relatively low fundamental amenities.

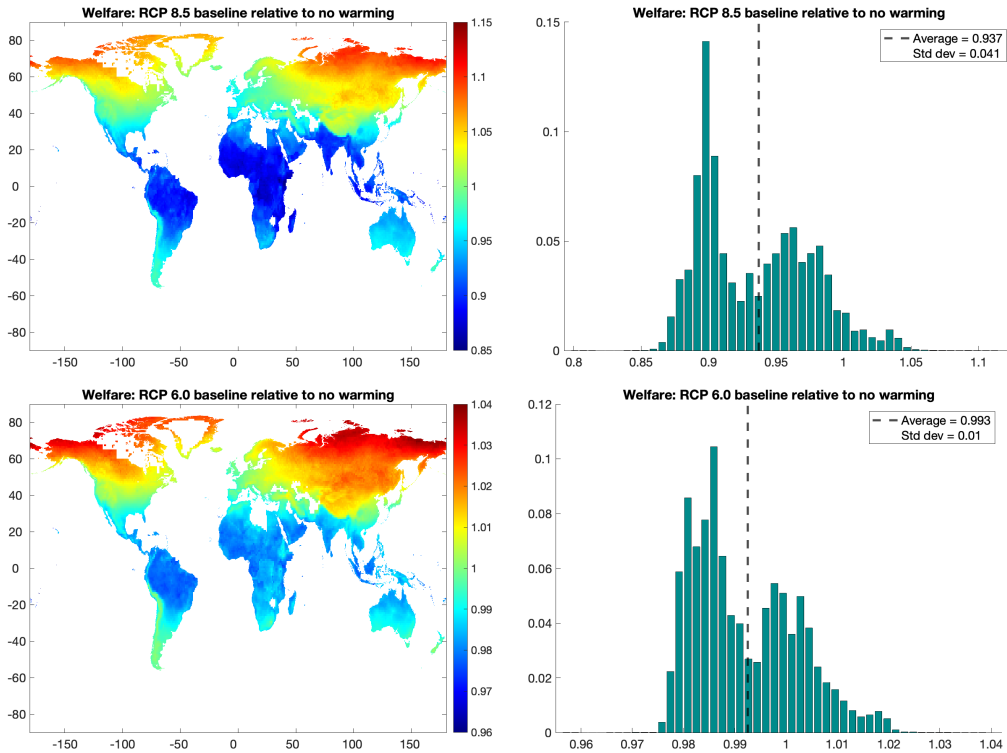


FIGURE 8
Welfare losses due to global warming.

of the cell also in 2000. The dashed black lines present the population-weighted linear relationship. The linear slope indicates that, on average, locations with double the level of real GDP exhibit welfare losses from global warming that are roughly 1.5 (0.2) percentage points lower in the RCP 8.5 (6.0) quantification. Hence, the poorest regions of the world, mainly located in Sub Saharan Africa and South East Asia, are expected to undergo the highest warming losses. OECD countries, with initially high income, are much less affected. China, with its vast and heterogeneous territory, displays regions with both high and low levels of welfare losses. Our results show that global warming will exacerbate the already large spatial inequality in the world.⁴⁸

It is interesting to decompose the effect of global warming by their source: amenity or productivity effects. In [Online Appendix F](#) we perform such an exercise and show that both effects are commensurate, although the effect on amenities is much more heterogeneous across space. Of course, as we underscore in the next subsection, there is tremendous uncertainty about the exact level of these aggregate losses, although there is much less uncertainty about their spatial distribution.

48. The correlation between current income and welfare losses from global warming is robust to different values of the elasticity of utility to real income. As argued in [Supplementary Materials Section L.4](#), lower values of this parameter modify the level of utility, but do not distort allocations. Hence, the slopes displayed in [Figure 9](#) are also positive, although smaller in magnitude, for lower values of the elasticity of utility to real income.

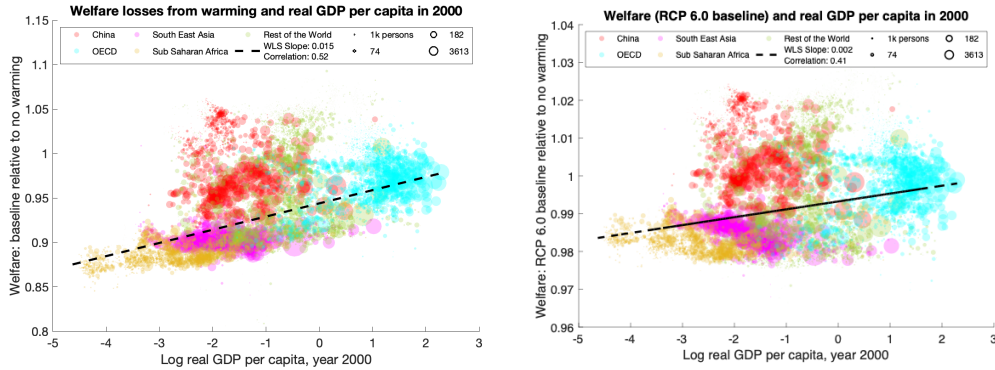


FIGURE 9
Correlation between welfare losses and initial real GDP per capita.

4.4. *Uncertainty*

Our baseline scenarios are computed using the logistic fit of the damage coefficients by temperature bin that we estimated in Section 3.2. As we discussed there, although we find evidence of significant temperature effects on amenities and productivity for locations with low and high temperatures, the estimation also yields large confidence intervals. The implied uncertainty embedded in the imprecise estimation of the damage functions translates into uncertainty about the effect that global warming will have on the economy. Hence, in this section, we evaluate the parametric uncertainty related to the imprecision in the estimation of the coefficients of the temperature damage functions for fundamental amenities and productivities.

Of course, we are also uncertain about many of the climate and economic parameters of the model as well as the model specification itself.⁴⁹ We address the uncertainty in the climate model by considering the two climate scenario calibrations we have been describing (RCP 8.5 and 6.0). Here, we also evaluate part of the parametric uncertainty in the economic model by analyzing the sensitivity of our results to the elasticity of substitution between energy sources, ϵ ; specifically, we calculate confidence intervals using the point estimate of 1.6 in Popp (2004) and letting the standard deviation be 0.56 as in Papageorgiou et al. (2017).

The top-left panel of Figure 10 presents the global average welfare losses over time in the baseline RCP 8.5 quantification (solid curve) and for damage functions determined by the logistic fit of the boundaries of the different confidence intervals, namely 60%, 80%, 90%, and 95%.⁵⁰ Baseline damages intensify through the next two centuries, with a peak of 10%. The figure illustrates how uncertain we are about the aggregate effect of global warming. The 95% confidence interval includes catastrophic welfare losses of as much as 20% by 2200 but also no losses (the 95% confidence interval for the RCP 6.0 quantification includes losses of 6% and gains of 0.5%). Confidence intervals widen

49. Desmet et al. (2018) performs a number of back-casting exercises that lend credibility to the long-run performance of the specification of the economic model.

50. Online Appendix E displays the corresponding graphs for the RCP 6.0 quantification. Supplementary Materials Sections J.1 and J.2 present the corresponding results for real GDP losses for both RCP quantifications.

during the first two centuries as temperature rises, but shrink slightly when temperature stabilizes and starts declining slowly.

The large uncertainty on aggregate losses does not translate into large uncertainty on local relative effects. The top-right panel of Figure 10 displays the spatial distribution of local welfare effects for the baseline RCP 8.5 quantification, the lower 95% confidence interval (i.e., the *worst-scenario*), and the upper 95% confidence interval (i.e., the *best-scenario*). The levels of the distributions are clearly different. In the worst-scenario of the RCP 8.5 (6.0) quantification, only a negligible part of the population, 0.003% (0.024%), experiences welfare gains. Whereas, in the best-scenario only 50.51% (19.44%) of the population undergoes welfare losses. However, the range, standard deviation, and shape of local losses remain roughly similar in all scenarios.⁵¹ This is the sense in which we are less uncertain about relative local effects than about the magnitude of average effects. In the baseline, as well as the best- and worst-scenarios, the losers from global warming are primarily Central America, Brazil, Africa and India.

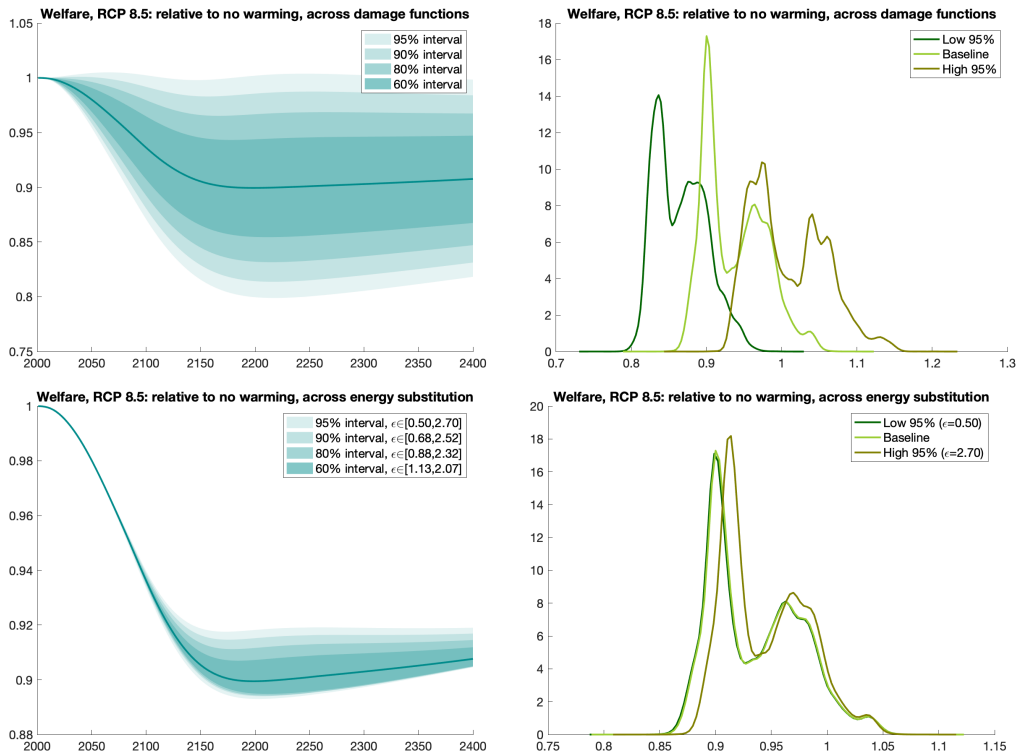


FIGURE 10

Uncertainty in welfare losses from damage functions and elasticity of substitution between energy sources.

51. As we move to more optimistic scenarios, the standard deviation of welfare losses tends to augment slightly. This is the result of the shape of the damage functions on amenities and productivities across different confidence levels. In the most pessimistic scenario, marginal damages are roughly constant in the hottest bins while they decline in the most optimistic scenario, as shown in Figure 2.

The bottom panels of Figure 10 present the uncertainty on welfare losses that results from parametric uncertainty about the elasticity of substitution between energy sources, ϵ , for the RCP 8.5 quantification. With higher ϵ , the economy substitutes more toward clean energy over time, as increases in world income result in improvements in clean energy technology, and cumulative emissions result in higher costs of fossil fuels. The less pronounced increase in CO₂ emission in turn restrains temperature increases. Due to the gradual nature of this process, the uncertainty on welfare losses resulting from uncertainty about ϵ is negligible during the first century. Over time, confidence intervals widen so that, by the end of the next century, average welfare losses range from 11% (3%) to 8% (1%) in the RCP 8.5 (6.0) quantification. As in the case of uncertainty in the damage function, the uncertainty on aggregate losses does not translate into meaningful uncertainty on local relative effects. In [Supplementary Materials Section L](#), we test the sensitivity of our results to many other parameters, including the discount factor, the concavity of the utility function, natality rates, and the size of fuel deposits. We also present exercises with more extreme values of ϵ , that might be relevant to assess scenarios where most machines (like cars) use electricity rather than fossil fuels.

5. ADAPTATION

In the model we have put forward, agents react to rises in temperatures by moving, trading, and investing in different locations on Earth. These adaptation mechanisms help agents cope with experienced changes in the environment. Modeling the effect of global warming using a micro-founded general equilibrium framework that incorporates these mechanisms allows us to assess the role of economic adaptation in shaping the economy's response. Of course, the extent to which agents use these adaptation channels depends on their cost. In this section, we evaluate the importance of the different mechanisms by comparing our baseline results with counterfactual scenarios where agents face higher migration, trade, or innovation costs. For conciseness, from now on we only present results for the RCP 8.5 quantification.

5.1. *Migration*

In the baseline scenario we set local migration costs such that the model accounts exactly for the distribution of local population changes between 2000 and 2005. Here, we consider global increases in migration costs by raising the migration cost function $m_2(\cdot)$ to a power $\vartheta > 1$, which corresponds to a proportional increase of size $\vartheta - 1$ if $m_2(\cdot)$ is close enough to one.⁵² Larger migration frictions imply that agents migrate less to the most productive locations, leading to lower incomes, energy and fossil fuel use, CO₂ emissions, and temperatures. Lower temperatures, in turn, increase productivity and amenities in some locations. In addition, since higher migration costs imply that agents remain in poor locations, and overall incomes are lower, natality rates are higher, leading to increases in population, aggregate fossil fuel consumption, and temperatures. These feedback mechanisms make the effect of migration costs quite complex.

Figure 11 presents the welfare impact of higher migration costs across space and over time. The left panel presents relative welfare with and without global warming

⁵² An alternative way to measure the relevance of migration as an adaptation mechanism is to change the variance of the idiosyncratic taste shock across locations, $1/\Omega$. In [Online Appendix G.1](#), we present the spatial and temporal impact of global warming when we reduce Ω .

in the baseline case with respect to relative welfare with and without global warming in the case with log migration costs that are 25% higher, that is, the difference-in-differences (DiD) effect of migration costs on the effect of temperature. Red areas in the figure represent locations where larger migration costs make global warming more costly (namely, the baseline is better). Clearly, higher migration costs hurt northern regions that tend to benefit from temperature rises by attracting migrants. In contrast, it benefits regions in Latin America, and especially Oceania, that are relatively sparsely populated and, in the baseline scenario, suffer large population losses and the correspondingly lower investments in technology due to global warming. Higher migration frictions help these places keep the critical population mass that is essential for development as they face larger temperatures. In contrast, and perhaps surprisingly, Central Africa, India, and China, all have larger losses from global warming when migration costs are large. The reason is that their high density and low income imply that much of the resulting increases in population concentrate there, leading to higher productivity growth but also lower wages and lower amenities due to congestion. In these regions, migration serves as a safety valve.⁵³ The latter effect dominates in dense developing countries, but the former dominates in sparsely populated regions, like Oceania.

The right panel of Figure 11 presents the evolution of average welfare losses over time. The dashed lines present the overall effects for two different magnitudes of ϑ . To help with the interpretation, we also present scenarios (solid lines) where we keep the evolution of temperature and population as in the baseline scenario. These exercises abstract from the feedback effect of temperatures and population on the economy. Comparing dashed and solid lines reveals the importance of these feedback effects. In the short-run, higher migration costs reduce economic activity leading to smaller temperature increases and smaller losses. In the long-run, in contrast, increases in population lead to more fossil fuel use, higher temperatures, and larger losses. Overall, larger migration costs lead to significantly larger losses from global warming. 25% larger migration costs lead to losses from temperature change that are about a third larger by 2200. Over time, these differences decline, since in all scenarios carbon reserves are eventually depleted.

These results show that migration is indeed an essential adaptation mechanism. One that is quantitatively important, but differentially across regions in the world. Ultimately, the best way to adapt to global warming is for agents to migrate to regions that lose less or even gain from temperature increases. Many of these regions are sparsely populated today, due to their lack of amenities and productivity, but could be improved as temperatures rise and new migrants invest in them over the next centuries.

Border Frictions. As a consequence of global warming, our model suggests a large reallocation of population over space, with a large population outflow from tropical areas into northern latitudes. Congestion and fears of a lack of cultural adaptation in the northern part of the world might create incentives for policymakers to rise the migration costs of moving to these regions, particularly for individuals coming from the developing world. For example, migrants from Africa, one of the regions more severely affected by global warming, might not be given permission to migrate legally to Europe or the U.S. To study this potential policy reaction, here we analyze the economic impact of global warming when the cost of moving from Africa to the rest of the world (RoW) increases,

53. The increase in population implied by this large change in migration costs is as large as 5.4 billion by 2150, stabilizing afterwards.

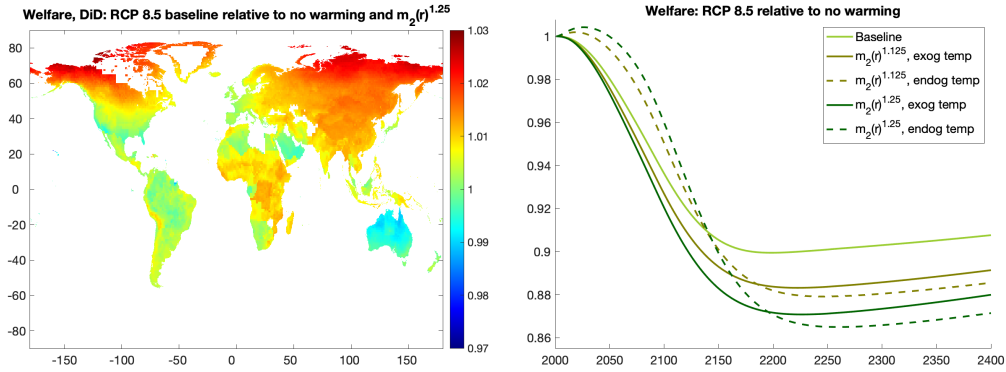


FIGURE 11
Welfare impact of climate change for alternative migration costs.

keeping migration costs within these regions as in the baseline.⁵⁴ Note the difference relative to our previous exercise, in which we homogeneously rose the migration costs in every location of the world; now we exclusively rise the migration cost of moving from one region to another.

Figure 12 presents the welfare impact of an increase in 25% in the cost of leaving Africa from any of its locations, $n_2(d)$. The left panel shows that northern regions and Africa itself are affected the most. Northern latitudes suffer because migrants, and a larger market size, are essential for their development. Africa is impaired because the higher population density exacerbates congestion and reduces wages. The spatial pattern is, in fact, similar to the case with homogeneous increase in migration costs in Figure 11, albeit with larger losses. The right panel of Figure 12 displays the evolution of welfare losses for Africa and the RoW. Conditional on the path of temperature and global population, both Africa and the RoW lose from closing the border in every period. More stringent border frictions restrict the ability of the world economy to adjust to climate change by shifting population from more to less affected areas. As with other migration frictions, border restrictions also decrease the aggregate size of the world economy, leading to less emissions and smaller damages. This last effect dominates in the short-run once we incorporate the endogenous response in temperatures.

5.2. Trade

As with migration costs, we study the effect of global increases in frictions that raise the bilateral iceberg trade costs $\zeta(\cdot, \cdot)$ to some power $\vartheta > 1$. Online Appendix G.3 presents these results and shows that larger trade costs have only a small effect on the losses from global warming. To understand this result, remember that gravity in trade implies that most trade flows are very local. Because increases in temperatures are spatially correlated, areas that trade significantly with each other tend to experience similar shocks. Hence trade is not an effective adaptation mechanism in this model.⁵⁵

54. In Online Appendix G.2, we describe the procedure to incorporate migration costs across a border. We also present an additional evaluation where we rise the costs of migrating from the developing into the developed world.

55. Importantly, our work abstracts from trade across industries due to local comparative advantage. If temperature affects sectors differentially and therefore the comparative advantage of regions, trade can

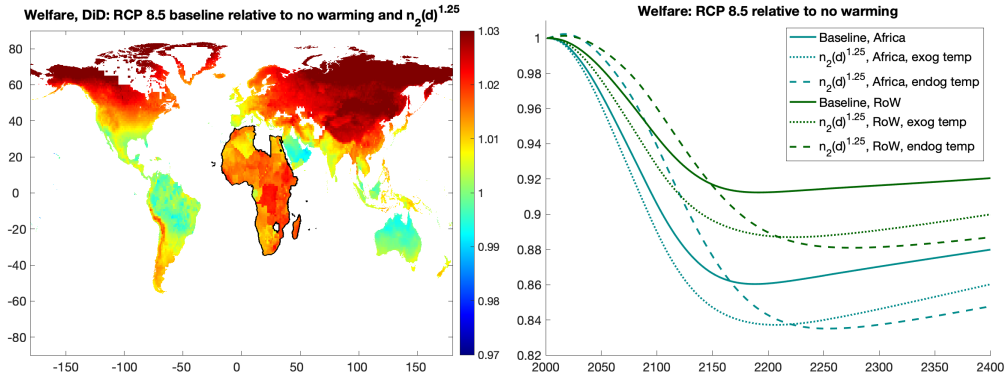


FIGURE 12

Welfare impact of climate change with higher costs of migrating from Africa to the RoW.

5.3. Innovation

The final adaptation mechanism we study in this section is innovation. Firm investments respond to market size and allow a region's technology to grow relative to that of other regions. We study the effect of rising the cost of innovation proportionally across locations. The utmost northern regions are hurt more (benefited less) by global warming when innovation costs are higher: developing these areas by improving their productivity and moving economic activity to the north becomes more costly. On aggregate, larger innovation costs lead to smaller losses from global warming. The reason is that larger innovation costs imply smaller benefits from density in locations that are eventually negatively affected by higher temperatures. In particular, Africa, India, and China experience lower technology growth and, therefore, attract fewer migrants from other locations. Given that these are the regions more affected by rising temperatures, the average cost from global warming declines. We present the specific results of this exercise in [Online Appendix G.4](#).

6. ENVIRONMENTAL POLICIES

Global warming constitutes a worldwide externality and so policy can potentially alleviate some of its negative economic impacts. Moreover, in the model we have proposed, there are local and global technological externalities, as well as congestion costs, all of which imply that the competitive equilibrium is not efficient. Hence, in this framework, achieving the first best would require a number of policies that address these other sources of inefficiencies as well. This is in general hard, since such policies would need local and global dynamic components that are currently unknown and, therefore, neither proposed nor implemented. In our framework, the market mechanisms that make the firm's innovation decision effectively static in the competitive equilibrium, do not apply to the planner's problem, which is fully forward looking and spatial. Hence, solving

play a much more important role as an adaptation mechanism. See [Desmet and Rossi-Hansberg \(2015\)](#), [Nath \(2020\)](#), [Conte et al. \(2021, 2022\)](#), and [Cruz \(2021\)](#) for studies that develop this mechanism. In [Online Appendix B.3](#) we do incorporate the local share of agriculture into the damage functions (although as a fixed local characteristic) and show that our results are not altered significantly.

for the optimal policy, even without considering global warming is, so far, beyond our capabilities. Thus, we proceed by evaluating some popular climate policies, rather than by designing optimal environmental policy.

A commonly proposed solution to the global carbon emission externality is to impose a global carbon tax, τ , to increase the cost of fossil fuels and discourage their use. This follows the standard Pigouvian logic of using taxes or subsidies to equate the social and private marginal cost of fossil fuels.⁵⁶ In the same spirit, we also consider a common and global clean energy subsidy, s , that reduces the marginal cost of renewable energy. Thus, the cost of energy per unit of land becomes $w_t(r)(1+\tau)Q_t^f(r)e_t^{f,\omega}(r) + w_t(r)(1-s)Q_t^c(r)e_t^{c,\omega}(r)$.⁵⁷ We assume that the balance of taxes and subsidies is taxed or rebated lump-sum at each location. Because carbon taxes delay the depletion of the stock of fossil fuels on Earth, we also study the potential gains from carbon taxes when an abatement technology is forthcoming.

6.1. Carbon Taxes

Figure 13 displays the evolution of CO₂ emissions and global temperatures when considering carbon taxes of 50%, 100% and 200%, keeping clean energy subsidies at zero.⁵⁸ We consider *ad-valorem* carbon taxes that are constant over time and space. As expected, carbon taxes reduce current consumption of fossil fuels at impact. For instance, a tax of 200% diminishes carbon emissions by 60% with respect to the baseline scenario in the initial period. However, as the economy grows and the productivity of energy production increases, CO₂ emissions rise. Eventually, though, extraction costs increase sharply, and so the price of fossil fuels relative to clean energy rises too, generating a decline in CO₂ emissions. Carbon taxes not only reduce initial emissions but they also delay the year and the magnitude of the peak in CO₂ emissions. For example, with a tax of 200% the peak is 2.53 GtCO₂ lower and occurs 36 years later than in the scenario with no carbon taxes.

In sum, the main effect of a carbon tax is to delay carbon consumption, by spreading its use over time; less current consumption but more future consumption. The more protracted path for CO₂ emissions has stark implications for the evolution of global temperatures: It *flattens* the temperature curve. A carbon tax of 200% leads to an evolution of average global temperature that is as much as 1.6°C lower in the first half of the 22nd century, peaks 46 years later at a temperature roughly 0.4°C lower, but eventually converges to the same temperature once the stock of carbon is depleted anyway. This intertemporal CO₂ utilization pattern, governed in part by the convex cost of carbon extraction relative to clean energy, is essential in determining the effectiveness of carbon taxes. Carbon taxes tend to delay, not eliminate, the use of fossil fuels (even when the elasticity of substitution between fossil fuels and clean energy is rather large, $\epsilon = 1.6$, as in our calibration).

56. See Hassler et al. (2019) for a modern treatment and quantification of Pigouvian logic applied to climate policy.

57. As already imposed in the notation and although potentially superior, we leave for future research an analysis of spatially heterogeneous policies or policies that vary over time. Such analysis is certainly feasible in our framework.

58. Given that the price of fossil fuels in the initial period is on average 73 usd/tCO₂, a carbon tax of 50% equals 37 usd/tCO₂, similar to the maximum in the E.U. Emissions Trading Scheme; and a carbon tax of 200% equals 146 usd/tCO₂, close to the Swedish tax, Hassler et al. (2020).

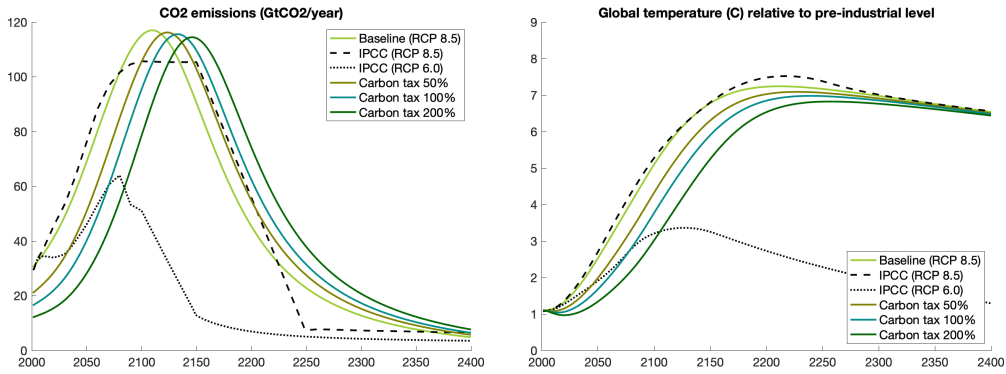


FIGURE 13
CO₂ emissions and global temperature under different carbon taxes.

Figure 14 presents global real GDP and welfare for each tax level relative to the baseline scenario with no environmental policy. At impact, the implementation of a uniform proportional carbon tax reduces the use of fossil fuels, which makes energy more expensive overall, and thus reduces income and welfare. The decline in welfare is less pronounced than that of real GDP, as welfare depends on real income which incorporates the lump-sum rebate. Furthermore, initially, carbon taxes reduce firm innovation since potential current profits decline, and therefore reduce the growth rate of the economy. Of course, as time evolves, the flattening of the temperature curve has beneficial effects on amenities and productivities, leading to higher real income and welfare, as well as higher growth rates. Eventually, the curves in Figure 14 cross one, meaning that the implementation of the carbon tax is, on average, beneficial after that period. In the long-run, real GDP and welfare keep increasing due to a larger global population.⁵⁹

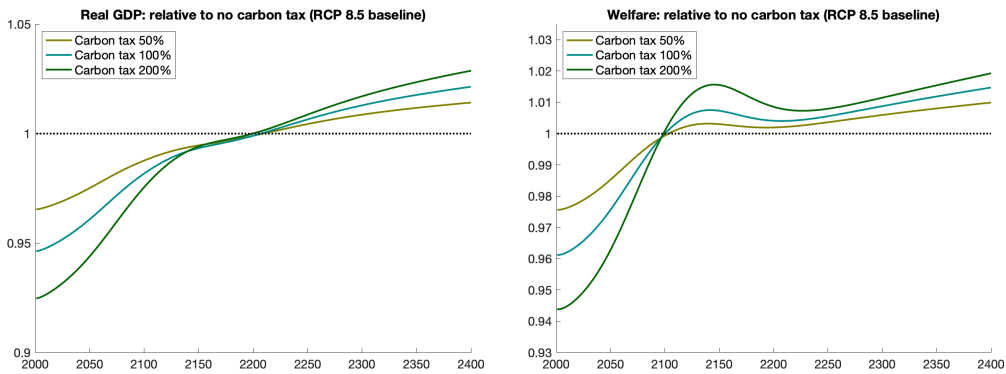


FIGURE 14
Real GDP and welfare under different carbon taxes.

The implementation of carbon taxes generates an intertemporal trade-off with short-term costs and long-term benefits. This naturally implies that any overall assessment

59. In the short-run, the implementation of carbon taxes reduces global income, augmenting natality rates.

TABLE 1
PDV of real GDP and welfare gains for different carbon taxes and discount factors.

	PDV of real GDP			Welfare		
	BGP growth rate	$\beta=0.965$	$\beta=0.969$	BGP growth rate	$\beta=0.965$	$\beta=0.969$
$\tau=0\%$ (RCP 8.5 base)	3.076%	1	1	2.971%	1	1
$\tau=50\%$	3.081%	0.993	1.028	2.974%	0.998	1.012
$\tau=100\%$	3.083%	0.990	1.044	2.977%	0.997	1.019
$\tau=200\%$	3.086%	0.986	1.063	2.979%	0.996	1.026

of carbon policies depends on the chosen discount factor. Table 1 presents the global average real GDP and welfare losses from global warming across different tax levels and discount factors, with respect to a scenario in which environmental policies are absent. Our choice of discount factor is limited by the BGP growth rate. In order to obtain finite present discounted values of welfare and real GDP for all future paths, we chose a baseline discount factor of $\beta=0.965$.⁶⁰ For this value, carbon taxes are not desirable today. The largest present discounted value of real GDP or welfare in Table 1 is obtained for $\tau=0$. However, if we increase the discount factor to $\beta=0.969$, a carbon tax of 200% or more maximizes welfare and real GDP. This large sensitivity of the optimal carbon tax is natural given the path shown in Figure 14 and cautions us not to rely too heavily on PDV statistics that depend on specific values of the discount factor. Ultimately, the discount factor determines the policymaker’s preferences for the welfare of current versus future generations. Regardless, carbon taxes result in large intertemporal transfers across generations.

The impact of carbon taxes is not only heterogeneous over time, but also across space. As expected, the regions that are projected to gain from imposing the carbon tax are the regions that were projected to lose the most from global warming in Figure 8. Welfare gains from a 200% carbon tax range from 3% in South America, Central Africa, and South Asia; to losses of 6% in the coldest places, those expected to gain from higher temperatures. Two interesting exceptions are the Middle East and Algeria. They obtain relatively low gains from the global carbon tax, compared to their projected losses from global warming. The economy of those regions relies heavily on fossil fuels, so a carbon tax generates large distortions in production.⁶¹

The previous exercise studies the effect of constant carbon taxes. Some proposals, as in Nordhaus (2017) and Dietz and Lanz (2019), suggest carbon taxes that increase over time. Figure 15 shows the impacts on CO₂ emissions and global temperature of a carbon tax of 50% increasing at zero, one, two, and three percent per year. In order to reduce the total amount of CO₂ emissions, and not only delay its consumption, we need to impose carbon taxes with a sufficiently high growth rate. For instance, with a growth rate of 3%, we achieve a reduction in the long-run level of temperature commensurate with the RCP 6.0 scenario. Note that the taxes needed to achieve this are quite large: 134% in the year 2100 and 362% in 2200.⁶²

60. We also consider a value of $\beta=0.969$ that, given the BGP growth rate of 0.03, implies that we value the relative gains in all periods similarly.

61. Online Appendix H.1 presents these results. Supplementary Materials Section N.2 evaluates the role of carbon taxes in the worst- RCP 8.5 scenario for climate damages and Supplementary Materials Section O.1 develops further the discussion on the temporal and spatial effects of carbon taxes.

62. Nordhaus and Yang (1996) considers also spatially uniform excise carbon taxes, expressed in dollars per ton of CO₂, rather than spatially uniform *ad-valorem* carbon taxes, expressed as a percentage of the price of fossil fuels. Supplementary Materials Section O.5 studies these alternative taxes and finds that constant spatially uniform excise carbon taxes again delay the consumption of fossil fuels and have

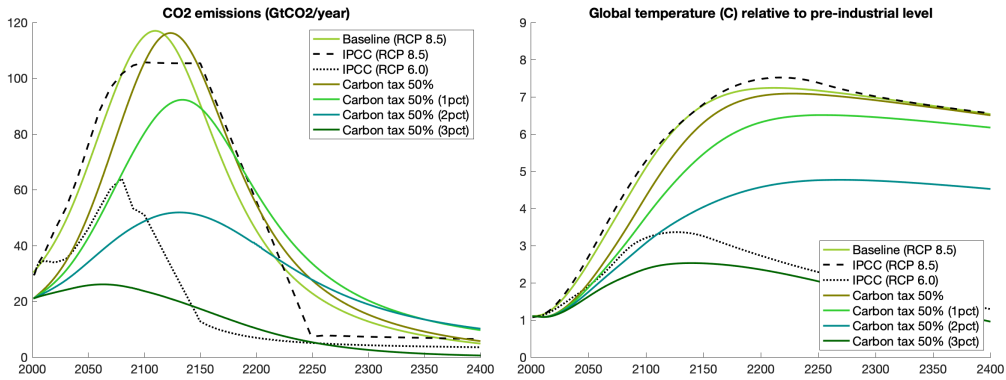


FIGURE 15
CO₂ emissions and global temperature with growing carbon taxes.

Obviously, we can reduce CO₂ total emissions to any desired level if we impose carbon taxes that grow sufficiently fast. However, the environmental benefit comes at an economic cost. The higher the growth rate of the carbon tax, the larger the distortion in production and, thus, the starker the trade-off between the short-run cost and the long-run benefit, as illustrated in Figure 16. In sum, carbon taxes that grow at a fast pace are useful when society values the future sufficiently.

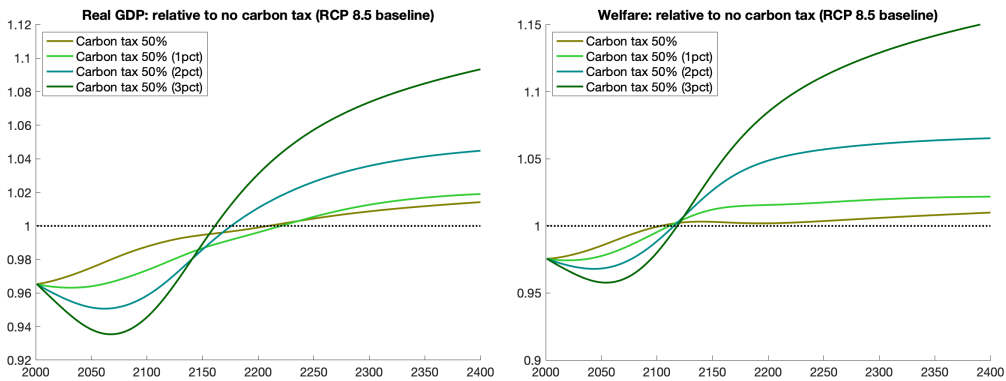


FIGURE 16
Real GDP and welfare with growing carbon taxes.

6.2. *Abatement*

We have shown that the main effect of carbon taxes is to delay the use of fossil fuels, without affecting the total stock of carbon released to the atmosphere, thereby *flattening* the evolution of global temperatures. Of course, delaying CO₂ emissions, and flattening the temperature curve can be extremely beneficial if, at some point, humans invent an

similar effects over space. Again, only if they grow at a sufficiently large rate do they help in reducing the total use of carbon.

TABLE 2
PDV of real GDP and welfare gains for different carbon taxes and discount factors with an abatement technology introduced in 2100.

	PDV of real GDP			Welfare		
	BGP growth rate	$\beta=0.965$	$\beta=0.969$	BGP growth rate	$\beta=0.965$	$\beta=0.969$
$\tau=0\%$ (RCP 8.5 base)	3.076%	1	1	2.971%	1	1
$\tau=50\%$	3.081%	0.997	1.044	2.974%	1.004	1.032
$\tau=100\%$	3.083%	0.996	1.072	2.977%	1.008	1.053
$\tau=200\%$	3.086%	0.995	1.107	2.979%	1.011	1.080

abatement technology that allows us to use fossil fuels without emitting CO₂ into the atmosphere (or capture CO₂ in the atmosphere through geoengineering). An abatement technology would eliminate, or reduce, the negative externality that results from the use of fossil fuels.⁶³ Since an abatement technology *cures* the economy from emitting CO₂ emissions after its invention, delaying the use of fossil fuels and flattening the temperature curve can become a very effective strategy, one that does affect total CO₂ emissions.⁶⁴ This is why carbon taxes and abatement technologies are complementary policies.

To illustrate this argument, here we consider a simple case in which an abatement technology becomes available at no cost in the year 2100.⁶⁵ Table 2 shows the global average PDV of real GDP and welfare gains under the implementation of carbon taxes when an abatement technology becomes available in 2100. When comparing it with Table 1, we observe that, when an abatement technology is forthcoming, large carbon taxes are beneficial for the economy for both discount factors. With $\beta=0.969$, the impact of this policy is very large and can yield gains in real GDP of 11% and in welfare of 8%. These results illustrate how the abatement technology and carbon taxes are complementary policies. That is, a forthcoming abatement technology makes carbon taxes a much more effective policy. In fact, this combination of policies is the most effective one we have found in our analysis.⁶⁶

6.3. Clean Energy Subsidies

Clean energy subsidies have two countervailing effects. First, they make clean energy less expensive, thereby creating incentives for agents to produce energy with clean sources. The magnitude of this effect is governed by the elasticity of substitution in energy

63. More precisely, if we denote by $\nu_t(r)$ the share of CO₂ emissions abated in region r at period t , the evolution of atmospheric CO₂, given by equation (2.13), becomes $S_{t+1} = S_{\text{pre-ind}} + \sum_{\ell=1}^{\infty} (1 - \delta_{\ell})(E_{t+1-\ell}^{fj} + E_{t+1-\ell}^x)$, where $E_t^{fj} = \int_S \int_0^1 (1 - \nu_t(v)) e_t^{f,\omega}(v) H(v) d\omega dv$. The law of motion of fossil fuel extraction is still given by equation (2.8).

64. The interaction of carbon taxes and an abatement technology within our framework is analogous to lockdowns and the introduction of a vaccine in a pandemic: a lockdown delays current infections at an economic cost, but reduces total infections only if a vaccine is forthcoming.

65. As in Nordhaus (2015), we could alternatively assume that preventing a share $\nu_t(r)$ of CO₂ emissions in region r at period t costs a fraction, $(1 - \varpi_{1,t}(r) \cdot \nu_t(r)^{\varpi_2})$, of household's income. We could assume that $\varpi_{1,t}(r)$ declines over time to reflect the widening menu of technological alternatives and that it varies across regions depending on their carbon intensity. The parameter ϖ_2 controls the degree of non-linearity in costs. At a global scale, Nordhaus (2015) considers $\varpi_{1,t} = 0.0334$ and $\varpi_2 = 2$. Of course, because of well-understood free-rider problems, the abatement policy would still need to be imposed by a global agreement.

66. Online Appendix H.2 presents the evolution of CO₂, temperature, real GDP and welfare with carbon taxes and an abatement technology that appears in 2100. Supplementary Materials Sections O.3 and O.4 show exercises with alternative measurements and timing.

production which we set at $\epsilon=1.6$, as well as by the initial relative productivity of clean energy, which is heterogeneous across locations and chosen to match relative energy use. Second, clean energy subsidies reduce the price of the energy composite. This additional effect is also governed by the share of clean energy in the energy composite, which is initially about 11%.

In the quantitative model we have put forward, these two effects roughly cancel out. Subsidies as large as 75% yield only a minuscule reduction in CO₂ emissions and temperatures.⁶⁷ We conclude that clean energy subsidies are not an effective way to combat global warming if the elasticity of substitution between energy sources is fixed and the innovation rate in clean energy does not respond to incentives. Incorporating directed technical change, as in [Hémous and Olsen \(2021\)](#), into our spatial integrated assessment model is challenging but relevant.

7. CONCLUSIONS

The goal of this paper is to propose a novel high-resolution spatially integrated assessment model (S-IAM) of the effect of global warming on economic outcomes and welfare. The large heterogeneity in projected temperature changes across regions of the world, and the heterogeneous effects of these changes across locations and over time, underscore the need for assessment models that feature a realistic geography with many locations and agents that make decisions to live, move, trade, and invest across them. The micro-founded spatial dynamic model that forms the core of the proposed framework features local population growth, costly migration and trade, endogenous technology investments, as well as local fossil and energy use and its impact on local temperature and, correspondingly, its heterogeneous effect on amenities and productivity levels. Thus, the proposed model allows us to incorporate a number of endogenous adaptation mechanisms that have been mostly absent in more aggregate assessment models so far. Furthermore, it allows us to estimate the overall impact of global warming on economic outcomes by explicitly aggregating the dynamic effects on local outcomes.

When we quantify the proposed economic model for the world economy at a fine level of spatial resolution we obtain local effects of global warming on welfare, in the baseline RCP 8.5 (6.0) quantification, that range from losses of 20% (4%) to gains of 11% (4%). Our results show that global warming will increase spatial inequality since, on average, countries with double the level of current real income experience welfare losses that are about 1.5 (0.2) percentage points lower. We find that the distribution of relative losses across locations is fairly robust to the damage functions we estimate but, in contrast, our estimates imply large uncertainty about overall welfare losses. The 95% confidence interval of average welfare losses in 2200 ranges from losses of 20% (6%) to zero. This wide range reflects that, although the data allows us to estimate significant effects of temperature on fundamental productivity and amenities, the estimates are still imprecise given that the rise in temperatures has only recently started to affect economic outcomes more severely.

The model we propose can be used as a workhorse model to study a number of additional dimensions of climate change as well as alternative policies. A few examples

67. [Online Appendix H.3](#) presents these results. It also presents additional results on clean energy subsidies including the evolution of carbon emissions and temperature, and the welfare effects across locations and over time. [Supplementary Materials Section O.2](#) evaluates the joint effect of carbon taxes and clean energy subsidies.

are coastal flooding, as analyzed in [Desmet et al. \(2021\)](#), the spatial effects of the increased likelihood of extreme weather events, or the political economy of climate policy as determined by the spatially heterogeneous effects we have uncovered.

Inevitably, our model abstracts from some important aspects. First, the model we propose introduces multiple sectors only in the estimation of the damage functions and as a fixed local characteristic. Adding endogenous specialization, as in [Conte et al. \(2021, 2022\)](#) or [Cruz \(2021\)](#), would enrich the role of trade as an adaptation mechanism. Second, we have abstracted from purposeful innovations in green, fossil, and abatement technologies. In our model, these technologies only evolve through spillovers from other innovations. Third, the model we develop gains tractability from assuming an economic structure in which anticipatory effects from future shocks or policy only affect land rents, but do not affect allocations. That is, future events do not affect the spatial evolution of the economy. Incorporating anticipatory effects in a rich spatial model with endogenous investments and growth is challenging, although potentially interesting. Of course, the importance of anticipatory effects to evaluate protracted phenomena, like global warming, is still debatable.⁶⁸

Global warming presents a daunting challenge for humanity. Designing the best tools to address it requires modern micro-founded economic models that incorporate multiple forms of adaptation and the rich spatial heterogeneity of the world. Our hope is that this paper contributes to this effort.

Acknowledgments. We thank Jordan Rosenthal-Kay, Cathy Wang, and Xiang Zhang for excellent research assistance. We also thank Thomas Chaney, Klaus Desmet, Martin Jégard, Per Krusell, three anonymous referees and numerous seminar participants for their feedback. We are grateful to the Ciriacy Wantrup Postdoctoral Fellowship at the University of California, Berkeley; the University of Chicago; and the International Economics Section at Princeton University for financial support.

Supplementary Data

Supplementary data are available at *Review of Economic Studies* online. And the replication package is available at <https://doi.org/10.5281/zenodo.7681424>.

Data Availability Statement

The data underlying this article are publicly available on Zenodo at <https://doi.org/10.5281/zenodo.7681424>.

REFERENCES

- Acemoglu, D., P. Aghion, L. Barrage, and D. Hémous (2020). Climate change, directed innovation and energy transition: The long-run consequences of the shale gas revolution.
- Acemoglu, D., P. Aghion, L. Bursztyn, and D. Hémous (2012, February). The environment and directed technical change. *American Economic Review* 102(1), 131–66.
- Acemoglu, D., U. Akcigit, D. Hanley, and W. Kerr (2016). Transition to clean technology. *Journal of Political Economy* 124(1), 52–104.
- Albouy, D., W. Graf, R. Kellogg, and H. Wolff (2016). Climate amenities, climate change, and american quality of life. *Journal of the Association of Environmental and Resource Economists* 3(1), 205–246.
- Allen, T. and C. Arkolakis (2014, 05). Trade and the topography of the spatial economy. *The Quarterly Journal of Economics* 129(3), 1085–1140.
- Anthoff, D. and R. Tol (2014). The climate framework for uncertainty, negotiation and distribution (fund), technical description, version 3.9.

68. There is some evidence showing that expectations about future climate change are being capitalized in agricultural land ([Severen et al., 2018](#)), housing ([Bernstein et al., 2019](#)), and municipal bonds ([Painter, 2020](#)).

- Auffhammer, M. (2018, November). Quantifying economic damages from climate change. *Journal of Economic Perspectives* 32(4), 33–52.
- Balboni, C. (2021). In harm's way? infrastructure investments and the persistence of coastal cities. *Working Paper*.
- Barrage, L. (2019, 10). Optimal Dynamic Carbon Taxes in a Climate–Economy Model with Distortionary Fiscal Policy. *The Review of Economic Studies* 87(1), 1–39.
- Barreca, A., K. Clay, O. Deschenes, M. Greenstone, and J. S. Shapiro (2016). Adapting to climate change: The remarkable decline in the us temperature-mortality relationship over the twentieth century. *Journal of Political Economy* 124(1), 105–159.
- Bauer, N., J. Hilaire, R. J. Brecha, J. Edmonds, K. Jiang, E. Kriegler, H.-H. Rogner, and F. Sferra (2017). Data on fossil fuel availability for shared socioeconomic pathways. *Data in Brief* 10, 44 – 46.
- Baylis, P. (2020). Temperature and temperament: Evidence from twitter. *Journal of Public Economics* 184, 104161.
- Becker, G. (1960). An economic analysis of fertility. In *Demographic and Economic Change in Developed Countries*, pp. 209–240. National Bureau of Economic Research, Inc.
- Benveniste, H., M. Oppenheimer, and M. Fleurbaey (2020). Effect of border policy on exposure and vulnerability to climate change. *Proceedings of the National Academy of Sciences*.
- Bernstein, A., M. T. Gustafson, and R. Lewis (2019). Disaster on the horizon: The price effect of sea level rise. *Journal of financial economics* 134(2), 253–272.
- Bosetti, V., E. Massetti, and M. Tavoni (2007). The WITCH Model. Structure, Baseline, Solutions. Climate Change Modelling and Policy Working Papers 12064, Fondazione Eni Enrico Mattei (FEEM).
- BP (2019). Bp statistical review of world energy.
- Burke, M., S. M. Hsiang, and E. Miguel (2015a). Climate and conflict. *Annual Review of Economics* 7(1), 577–617.
- Burke, M., S. M. Hsiang, and E. Miguel (2015b). Global non-linear effect of temperature on economic production. *Nature* 527, 235–239.
- Carleton, T., A. Jina, M. Delgado, M. Greenstone, T. Houser, S. Hsiang, A. Hultgren, R. E. Kopp, K. E. McCusker, I. Nath, J. Rising, A. Rode, H. K. Seo, A. Viaene, J. Yuan, and A. T. Zhang (2022, 04). Valuing the Global Mortality Consequences of Climate Change Accounting for Adaptation Costs and Benefits*. *The Quarterly Journal of Economics* 137(4), 2037–2105.
- Casey, G., S. Shayegh, J. Moreno-Cruz, M. Bunzl, O. Galor, and K. Caldeira (2019, may). The impact of climate change on fertility. *Environmental Research Letters* 14(5), 054007.
- Conley, T. (1999). Gmm estimation with cross sectional dependence. *Journal of Econometrics* 92(1), 1 – 45.
- Conte, B., K. Desmet, D. K. Nagy, and E. Rossi-Hansberg (2021, 09). Local sectoral specialization in a warming world. *Journal of Economic Geography* 21(4), 493–530.
- Conte, B., K. Desmet, and E. Rossi-Hansberg (2022, November). On the geographic implications of carbon taxes. Working Paper 30678, National Bureau of Economic Research.
- Costinot, A., D. Donaldson, and C. Smith (2016). Evolving Comparative Advantage and the Impact of Climate Change in Agricultural Markets: Evidence from 1.7 Million Fields around the World. *Journal of Political Economy* 124(1), 205–248.
- Crippa, M., G. Oreggioni, D. Guizzardi, M. Muntean, E. Schaaf, E. Lo Vullo, E. Solazzo, F. Monforti-Ferrario, J. G. Olivier, and E. Vignati (2019). Fossil co2 and ghg emissions of all world countries. *Publication Office of the European Union: Luxembourg*.
- Crippa, M., E. Solazzo, G. Huang, D. Guizzardi, E. Koffi, M. Muntean, C. Schieberle, R. Friedrich, and G. Janssens-Maenhout (2019). High resolution temporal profiles in the emissions database for global atmospheric research (edgar). *Nature Scientific Data*.
- Cruz, J.-L. (2021). Global warming and labor market reallocation. *Working Paper*.
- Cruz, J.-L. and E. Rossi-Hansberg (2022, May). Local carbon policy. (30027).
- Dell, M., B. F. Jones, and B. A. Olken (2012, July). Temperature shocks and economic growth: Evidence from the last half century. *American Economic Journal: Macroeconomics* 4(3), 66–95.
- Dell, M., B. F. Jones, and B. A. Olken (2014). What do we learn from the weather? the new climate–economy literature. *Journal of Economic Literature* 52(3), 740–798.
- Delventhal, M. J., J. Fernández-Villaverde, and N. Guner (2021). Demographic transitions across time and space. Technical report, National Bureau of Economic Research.
- Deschênes, O. and M. Greenstone (2007, March). The economic impacts of climate change: Evidence from agricultural output and random fluctuations in weather. *American Economic Review* 97(1), 354–385.
- Desmet, K., R. E. Kopp, S. A. Kulp, D. K. Nagy, M. Oppenheimer, E. Rossi-Hansberg, and B. H. Strauss (2021). Evaluating the economic cost of coastal flooding. *American Economic Journal: Macroeconomics*.
- Desmet, K., D. Nagy, and E. Rossi-Hansberg (2018). The geography of development. *Journal of Political Economy* 126(3), 903–983.
- Desmet, K. and E. Rossi-Hansberg (2014, April). Spatial development. *American Economic Review* 104(4), 1211–43.

- Desmet, K. and E. Rossi-Hansberg (2015). On the spatial economic impact of global warming. *Journal of Urban Economics* 88(C), 16–37.
- Dietz, S. and B. Lanz (2019). Can a growing world be fed when the climate is changing? *SSRN 3507257*.
- Dietz, S., F. van der Ploeg, A. Rezai, and F. Venmans (2021). Are economists getting climate dynamics right and does it matter? *Journal of the Association of Environmental and Resource Economists* 8(5), 895–921.
- Eaton, J. and S. Kortum (2002). Technology, geography, and trade. *Econometrica* 70(5), 1741–1779.
- Fried, S. (2022). Seawalls and stilts: A quantitative macro study of climate adaptation. *The Review of Economic Studies* 89(6), 3303–3344.
- Golosov, M., J. Hassler, P. Krusell, and A. Tsyvinski (2014). Optimal taxes on fossil fuel in general equilibrium. *Econometrica* 82(1), 41–88.
- Graff-Zivin, J. and M. Neidell (2014). Temperature and the allocation of time: Implications for climate change. *Journal of Labor Economics* 32(1), 1–26.
- Hassler, J., B. Carlén, J. Eliasson, F. Johnsson, P. Krusell, T. Lindahl, J. Nycander, Åsa Romson, and T. Sterner (2020). Sns economic policy council report 2020: Swedish policy for global climate.
- Hassler, J., P. Krusell, and C. Olovsson (2018). The consequences of uncertainty: Climate sensitivity and economic sensitivity to the climate. *Annual Review of Economics* 10(1), 189–205.
- Hassler, J., P. Krusell, and C. Olovsson (2019, July). Directed technical change as a response to natural-resource scarcity. Working Paper Series 375, Sveriges Riksbank (Central Bank of Sweden).
- Hémous, D. and M. Olsen (2021). Directed technical change in labor and environmental economics. *Annual Review of Economics* 13(1), 571–597.
- Hope, C. and M. Hope (2013). The social cost of co 2 in a low-growth world. *Nature Climate Change* 3, 722–724.
- IEA (2019). *World Energy Outlook 2019*. IEA, Paris.
- IPCC (2007). Climate change 2007: Synthesis report. contribution of working groups i, ii and iii to the fourth assessment report of the intergovernmental pan on climate change. *Cambridge University Press*.
- IPCC (2013). Climate change 2013: The physical science basis. contribution of working group i to the fifth assessment report of the intergovernmental panel on climate change. *Cambridge University Press*.
- Joos, F., R. Roth, J. S. Fuglestedt, G. P. Peters, I. G. Enting, W. von Bloh, V. Brovkin, E. J. Burke, M. Eby, N. R. Edwards, T. Friedrich, T. L. Frölicher, P. R. Halloran, P. B. Holden, C. Jones, T. Kleinen, F. T. Mackenzie, K. Matsumoto, M. Meinshausen, G.-K. Plattner, A. Reisinger, J. Segsneider, G. Shaffer, M. Steinacher, K. Strassmann, K. Tanaka, A. Timmermann, and A. J. Weaver (2013). Carbon dioxide and climate impulse response functions for the computation of greenhouse gas metrics: a multi-model analysis. *Atmospheric Chemistry and Physics* 13(5), 2793–2825.
- Krusell, P. and J. Smith, Anthony A (2022, August). Climate change around the world. Working Paper 30338, National Bureau of Economic Research.
- Kummu, M., M. Taka, and J. Guillaume (2018, 02). Gridded global datasets for gross domestic product and human development index over 1990–2015. *Scientific Data* 5, 180004.
- Lucas, R. E. (1976). Econometric policy evaluation: A critique. *Carnegie-Rochester Conference Series on Public Policy* 1, 19 – 46.
- Mcglade, C. and P. Ekins (2015, 01). The geographical distribution of fossil fuels unused when limiting global warming to 2c. *Nature* 517, 187–90.
- Missirian, A. and W. Schlenker (2017). Asylum applications respond to temperature fluctuations. *Science* 358(6370), 1610–1614.
- Mitchell, T. (2003). Pattern scaling: An examination of the accuracy of the technique for describing future climates. *Climatic Change* 60, 217–242.
- Myhre, G., E. J. Highwood, K. P. Shine, and F. Stordal (1998). New estimates of radiative forcing due to well mixed greenhouse gases. *Geophysical Research Letters* 25(14), 2715–2718.
- Nath, I. B. (2020). The food problem and the aggregate productivity consequences of climate change. Technical report, National Bureau of Economic Research.
- Nordhaus, W. (2006). Geography and macroeconomics: New data and new findings. *Proceedings of the National Academy of Sciences* 103(10), 3510–3517.
- Nordhaus, W. (2015, April). Climate clubs: Overcoming free-riding in international climate policy. *American Economic Review* 105(4), 1339–70.
- Nordhaus, W. (2017). Revisiting the social cost of carbon. *Proceedings of the National Academy of Sciences* 114(7), 1518–1523.
- Nordhaus, W. and J. Boyer (2002). Warming the world: Economic models of global warming. mit press, cambridge mass., 2000. isbn 0 262 14071 3. *Environment and Development Economics* 7(3), 593–601.
- Nordhaus, W. and X. Chen (2016). Global gridded geographically based economic data (g-econ), version 4. *NASA Socioeconomic Data and Applications Center (SEDAC)*.

- Nordhaus, W. D. and Z. Yang (1996). A regional dynamic general-equilibrium model of alternative climate-change strategies. *The American Economic Review* 86(4), 741–765.
- Painter, M. (2020). An inconvenient cost: The effects of climate change on municipal bonds. *Journal of Financial Economics* 135(2), 468–482.
- Papageorgiou, C., M. Saam, and P. Schulte (2017). Substitution between clean and dirty energy inputs: A macroeconomic perspective. *The Review of Economics and Statistics* 99(2), 281–290.
- Popp, D. (2004). Entice: endogenous technological change in the dice model of global warming. *Journal of Environmental Economics and Management* 48(1), 742 – 768.
- Popp, D. (2006). Entice-br: The effects of backstop technology r&d on climate policy models. *Energy Economics* 28(2), 188 – 222.
- Redding, S. J. and E. Rossi-Hansberg (2017). Quantitative spatial economics. *Annual Review of Economics* 9(1), 21–58.
- Rogner, H.-H. (1997). An assessment of world hydrocarbon resources. *Annual Review of Energy and the Environment* 22(1), 217–262.
- Rohde, R. A. and Z. Hausfather (2020). The berkeley earth land/ocean temperature record. *Earth System Science Data* 12(4), 3469–3479.
- Schlenker, W. and M. J. Roberts (2009). Nonlinear temperature effects indicate severe damages to u.s. crop yields under climate change. *Proceedings of the National Academy of Sciences* 106(37), 15594–15598.
- Severen, C., C. Costello, and O. Deschenes (2018). A forward-looking ricardian approach: Do land markets capitalize climate change forecasts? *Journal of Environmental Economics and Management* 89, 235–254.
- Stern, D. I. (2012). Interfuel substitution: A meta-analysis. *Journal of Economic Surveys* 26(2), 307–331.
- UN (2004). The united nations on world population in 2300. *Population and Development Review* 30(1), 181–187.
- UN (2019). *World Population Prospects 2019: Data Booklet*.
- USGCRP (2018). Impacts, risks, and adaptation in the united states: Fourth national climate assessment, volume ii.